Recent progress in nanomaterial-based assay for the detection of phytotoxins in foods

Chen, Qilei; Zhu, Lin; Chen, Jiaxuan; Jiang, Tao; Ye, Huazhen; Ji, Hong; Tsang, Siuwai; Zhao, Zhongzhen; Yi, Tao; Chen, Hubiao

Published in:
Food Chemistry

DOI:
10.1016/j.foodchem.2018.10.075

Published: 30/03/2019

Document Version:
Peer reviewed version

Recent progress in nanomaterial-based assay for the detection of phytotoxins in foods

Qilei Chen[a,†], Lin Zhu[a,†], Jiaxuan Chen[b], Tao Jiang[b], Huazhen Ye[c], Hong Ji[d], Siuwai Tsang[a], Zhongzhen Zhao[a], Tao Yi[a,*], Hu-Biao Chen[a,*]

[a] *School of Chinese Medicine, Hong Kong Baptist University, Hong Kong Special Administrative Region, 999077, P.R. China;*

[b] *College of Chemistry, Leshan Normal College, Leshan 614004, China;*

[c] *Department of pharmacy, Fujian Health College, Fuzhou 350101, China;*

[d] *School of Pharmaceutical Science, Guangzhou Medical University, Guangzhou, 511436, P.R. China.*

[†] These authors contribute equally to the work.

[*] Corresponding authors. Tel.: +852 3411 2081; fax: +852 3411 2461 (T. Yi); Tel.: +852 3411 2060; fax: +852 3411 5571 (H.B. Chen). E-mail addresses: yitao@hkbu.edu.hk (T. Yi); hbchen@hkbu.edu.hk (H.B. Chen).

Abstract

Phytotoxins refers to toxic chemicals derived from plants. They include both secondary metabolites that are dose-dependently toxic and allergens that can cause anaphylactic shock in sensitive individuals. Detecting phytotoxins in foods is increasingly important. Conventional methods for detecting phytotoxins lack sufficient sensitivity and operational convenience. Nanomaterial-based determination assays show great competence in fast and accurate sensing of trace substances. In the present review, representative phytotoxin categories of alkaloids, cyanides, and proteins are discussed. Application of notable nanomaterials, *e.g.* carbon nanotubes, graphene oxide, magnetic nanoparticles, metal-based nanotools, and quantum dots, in specific sensing strategies to fit the physiochemical properties of the target toxins are summarized. Nanomaterials mainly play four roles in phytotoxin detection: 1) analyte enricher; 2) sensor structure mediator; 3) target recognizer or reactant; 4) signaling agent. Great achievements have been made in the detection of trace plant-derived toxins in food matrices, yet there are still challenges awaiting further investigation.

Keywords

Nanomaterials; nanoparticles; graphene oxide; carbon nanotubes; toxins; food safety.

1. Introduction

Phytotoxins are chemicals produced by plants that can be toxic to humans. Some of these chemicals are secondary metabolites, such as alkaloids, cyanides, terpenes, and phenolics (Shibamoto & Bjeldanes, 2009). Other of these chemicals are vital to the growth and reproduction of the plant. For some phytotoxins, toxicity depends on dosage: at lower doses the chemical may be prophylactic or beneficial to humans, while toxic at higher doses. Other phytotoxins may elicit allergic reactions (Mcl Mowat, 2003). In both cases, the effects are often selective; that is, different people experience different and/or different levels of symptoms.

The phytotoxins can be retained throughout the processing of plant-derived foods and finally be ingested; thus, they are potential health hazards to humans. For example, methylxanthines of caffeine, theobromine, and theophylline are abundantly found in cocoa beans and tea, and are therefore frequently present in cookies, chocolate, and various beverages (Yingzi Wang, Ding, Li, & Hu, 2018). They stimulate the central nervous system and may lead to convulsions in high doses. Brucine and strychnine are two predominant terpene indole alkaloids commonly found in parts of the *Strychnos nux-vomica* tree. The two alkaloids are neurotoxic and may cause muscle spasms and multiple organ failures when inhaled or ingested my mistake (Gleason, Gosselin, & Hodge, 1957; Migliaccio, Celentano, Viglietti, & Viglietti, 1990). Opiates such as morphine and codeine are naturally found in a number of plants, most primarily in opium poppy (*Papaver somniferum*). The poppy seeds are often pressed to release poppyseed oil, which are used into meal as an ingredient in pastry and bread, more often in central Europe (Hensperger, 2001). The opiates are primarily used as pain medications; however, therapy may come with adverse effects such as constipation and hormone imbalance. If overdosed, one can suffer from asphyxia and even die of respiratory depression (Pfizer Pharmaceuticals Group, 2006). Some plants such as sorghum and cassava contain cyanogenic glycoside, which is enzymatically converted to cyanides after cell rupture. Cyanide is highly toxic to mammals by binding to a_3 cytochromes and inhibiting electron transport chain in mitochondria, in turn leading to a series of neurological problems (C.-Y. Liu & Tseng, 2011). Ricin and abrin are both type II ribosome-inactivating proteins naturally presenting in bean plants of *Ricinus communis* and *Abrus precatorius*, respectively. Once internalized into human cells, the biotoxins can inhibit protein synthesis and result in eventual cell death (Hu et al., 2015). Gliadin

in wheat, which represents approximately half of the wheat gluten protein and can cause anaphylaxis and even celiac disease in certain individuals (H. Y. Yin, Chu, Tsai, & Wen, 2016). Allergenic proteins of peanuts (*Arachis hypogaea*) include Ara h 1 (cupin; vicillin-type 7S globulin), Ara h 2 (conglutin; 2S albumin), Ara h 3 (cupin; legumin- type, 11S globulin), and Ara h 6 (conglutin; 2S albumin). They are accounted for a majority of allergic reactions to peanut (Weng & Neethirajan, 2016).

Widely applied techniques to detect the above toxins include high-performance liquid chromatography coupled with diode array detector (HPLC-DAD) (H. F. Zhang & Shi, 2012), gas chromatography coupled with mass spectrometry (Zhu et al., 2016), and capillary electrophoresis (Thabano, Breadmore, Hutchinson, Johns, & Haddad, 2009). However, these approaches usually involve tedious sample pretreatment, sophisticated instrument operation, and skilled manpower. More importantly, perhaps, it is not easy for such methods to be sensitive enough to detect trace amount of substances from a complicated sample mixture, *e.g.* food matrices, and in some cases it is trace amounts that have anaphylactic effects or high toxicity. Reports have been made, and regulations have been passed by various national food regulatory bodies, setting lethal dosage and exposure limits for some of these hazardous chemicals (Table 1). It is of great importance to establish efficient and sensitive techniques for food safety assessment.

Nanotechnology has made considerable progress in recent decades. Magnetic nanoparticles (MNPs) (Feng et al., 2015), metal nanomaterials (Y. Liu, Ai, Cheng, Huo, & Lu, 2010), carbon nanotubes (CNTs) (S. Yang et al., 2010), graphene oxide (GO) (Sereshti, Khosraviani, Samadi, & Amini-Fazl, 2014), and quantum dots (QDs) (C. Zhang et al., 2017) are among popular nanomaterials used for detecting phytotoxins in complex food matrices. These novel materials have large surface area and unique physicochemical properties that enhance the sensitivity, selectivity, and accuracy of the toxin analyses.

The present review summarizes recent progress in food phytotoxin detection by biosensors coupled with nanomaterials. Alkaloids, cyanides, and proteins, as well as their corresponding DNAs, are featured analytes. Various determination strategies in which target-specific sensing patterns are

drawn are evaluated. Nanomaterials participate in different phases of sample analysis; some materials are promising multifunctional detection agents due to their special properties. Challenges and possible solutions are discussed, with an expectation that more sophisticated nanomaterial-based sensing techniques contributing to food safety and public health will be developed in coming years.

Insert Table 1 here

2. Alkaloids

2.1. Analyte enrichment

Sensitive detection of alkaloids which are usually at low levels in plants calls for high extraction efficiency and isolation selectivity. Conventional alkaloid extractants include acidic water (Dar, Brahman, Tiwari, & Pitre, 2012; L. Yang et al., 2016) and alcohols (Behpour, Ghoreishi, Khayatkashani, & Motaghedifar, 2011; Behpour, Ghoreishi, Khayatkashani, & Motaghedifard, 2012). Following the extraction process, solid-phase extraction (SPE) is a frequently applied separation technique with integrated features of liquid-liquid extraction and column liquid chromatography (Hennion, 1999). In order to improve compound isolation from food matrices, there has been a growing interest in designing SPE sorbents as well as other separation-assisting agents with nanostructured materials, e.g. CNTs, MNPs, GO, Si-based NPs and Zn-based NPs (Augusto, Hantao, Mogollón, & Braga, 2013).

Multi-walled carbon nanotubes (MWCNTs) are among the most widely used carbon nanomaterial-based SPE sorbents. MWCNTs have high sorption capacity, due to their high surface area, as well as fine chemical and thermal stability, which make them suitable SPE packing materials (Feng et al., 2015). A cationic surfactant, hexadecyl-trimethylammonium bromide (HTAB), can interact with oxygen-containing functional groups of oxidized MWCNTs and thus is capped on the carbon nanomaterials as admicelles. For example, HTAB-MWCNT SPE sorbent has been used to determine caffeine levels in drinks. The sorbet is applied to preconcentrate caffeine from the test solution to a nylon membrane filter; the analyte subsequently enhances the fluorescence signal emitted by a fluorophore dye. The enhancement of the solid-surface

fluorescence (SSF) is in linear proportion to the concentration of caffeine in the test solution (Talio, Acosta, Alesso, Luconi, & Fernández, 2014).

A problem with using MWCNTs as SPE cartridge packing material is that it takes a long time and a substantial amount of organic solvents to desorb the target analytes from the sorbents. To speed up sample pretreatment and thereby resolve this issue, MNPs can be used to fabricate the MWCNTs. Instead of packing Fe_3O_4-enclosed hydroxylated MWCNTs (Fe_3O_4-MWCNTs-OH) into a cartridge, Feng et al dispersed the nanomaterials into a microvolume of an analysis solution containing strychnine. The sorbents were well dispersed in the solution due to their hydrophilicity. The target species were quickly adsorbed on the surface of the MWCNTs; the extraction efficiency was in turn enhanced. When the extraction was finished, the target-loaded magnetic MWCNTs were collected from the sample mixture under an external magnetic field. Accumulated strychnine was then eluted by a small volume of desorption organic solvent and determined by HPLC-DAD (Feng et al., 2015). Another magnetic solid phase microextraction (m-SPME) was successfully achieved by Fe_3O_4-MWCNTs combined with screen-printed carbon electrode (SPCE) to detect caffeine in drink samples (Filik & Aslıhan Avan, 2018). In summary, MNP-fabricated MWCNTs can make phase separation easy by eliminating tedious centrifugation and filtration steps; it has thus proved to be a novel SPE material for analyte enrichment.

m-SPME can also be achieved by linking MNPs with other drug-loading materials. For instance, MNPs can be capped with zinc-based metal organic framework-5 [MOF-5(Zn)], *i.e.* with zinc ions and organic bridging ligands together providing large porosity, tunable shape, and high surface area. MOFs are promising drug carriers owing to their high loading capacity, biodegradation ability and versatile functionality (Gaudin et al., 2012). Bahrani et al found that colchicine could be efficiently adsorbed on MOF-5(Zn)-Fe_2O_4 NPs, mainly due to ionic bonding between Zn^{2+} in MOF-5 and Fe^{3+} in Fe_2O_4 with methoxy groups of the alkaloid molecules. Besides, researchers have used ultrasound waves to accelerate mass transfer of the target analyte onto the adsorbents, increasing extraction efficiency. As a result, the MOF-5(Zn)-Fe_2O_4 NPs have been successfully applied in ultrasound assisted dispersive (UAD) m-SPME analysis of colchicine in autumn and spring roots of *Colchicum persicum* (Bahrani et al., 2017).

GO is another superior carbon-based SPE adsorbent with outstanding surface area (theoretical value 2630 m^2/g) and rich functional groups for chemical interaction (Sereshti et al., 2014). It has two major advantages compared to CNTs. Firstly, the planar sheets of GO favor molecule adsorption, while the inner walls of CNTs may have steric hindrance that prevents compound access. Secondly, it is easier to obtain pure GO, as it is synthesized directly from graphite, while CNTs usually contain trace amounts of metallic impurities that come from the metal catalysts used in the synthesis process, and these impurities may have negative influences (Q. Liu et al., 2011). An application of GO as a sorbent in UAD-SPME coupled with HPLC-UV to simultaneously detect theophylline, theobromine, and caffeine in tea beverages proved the nanosheet-based sample pretreatment method is practical and convenient (Sereshti et al., 2014). Besides working as an SPE sorbent, GO can assist chemical separation in a capillary electrophoresis (CE) analysis when used to coat the inner face of the capillary. The immobilized GO can act as a stationary phase to adjust the electroosmotic flow and improve the resolution by various mechanisms including electrostatic interactions, π–π interactions, and hydrogen bonding. In a simultaneous determination of three alkaloids in *Flos daturae* extract, the analytes were baseline separated under the optimal GO-coated CE-DAD conditions. However, the three targets were eluted out into one single peak on the chromatogram when an uncoated capillary was used under the same conditions (Ye, Li, Gao, & Xie, 2013).

The interior structure of the sorbents can be functionalized to achieve specific molecular recognition. A pore-engineered nanocarbon, carbon nanocage (CNC) was synthesized by using cage-type mesoporous silica KIT-5 as a hard template, resulting in regularly structured interior pores, giving high selectivity for tea components, including caffeine (Ariga, Vinu, Miyahara, Hill, & Mori, 2007). With a similar concept, silica nanoparticles (Si NPs) were used as templates to irradiate methacrylate polymer monoliths, increasing interior deprotonated carboxylate sites that bind to protonated basic analytes (e.g. caffeine). Consequently, the analyte adsorption capacity was boosted by 10 times. Such monolith templating has proved useful for preconcentrating and separating analytes by in-line SPE-CE (Thabano et al., 2009).

Polyacrylic acid-functionalized porous zinc sulfide nanospheres (PAA-PZNs) can also be chosen as

SPE sorbents. The assembled nanospheres have abundant carboxyl groups that can effectively concentrate alkaloids and have weak hydrophobic interaction with non-alkaloids (Zhu et al., 2015). In a specific enrichment and identification of alkaloids from *Crinum asiaticum var. sinicum* crude extracts, peak areas of lycoline, the external standard, calculated using the ZnS-based SPE method were higher than that quantified by commercial GP resin-based Classic PCX SPE, with rates of 1.9 and 1.5 for LC-MS and GC-MS detections, respectively (Zhu et al., 2016). The high yields of analytes proved that PAA-PZNs are strong sorbents for selective enrichment of alkaloids.

2.2. Electrode surface modification in electrochemical determination

2.2.1. Decorated carbon nanomaterials

Network-like graphene (Gr) and porous carbon nanotubes (CNTs) are among the most popular carbon nanomaterials assisting electrochemical determination of trace analytes, especially those with analogue structures, due to their large surface area and strong mechanical strength, providing abundant reaction sites and enabling efficient electron transfer (Savalia & Chatterjee, 2017; J. Y. Sun, Huang, Wei, Wu, & Ren, 2011). They are frequently used as electrode coatings to improve detection selectivity and sensitivity (Table 2). Furthermore, they can be capped by other materials for electrode fabrication. For instance, nitrogen has a comparable atomic size and similar valence electron layer structure with carbon; therefore it is a favorable conductivity-enhancing dopant on electronic biosensors (Ghosh, Kumar, Maruyama, & Ando, 2010). A study assembled nitrogen-doped Gr (N-Gr) and nitrogen-doped CNTs (N-CNTs) into nanocomposites to modify the surface of a glassy carbon electrode (GCE) via electrodeposition to detect caffeine and vanillin in cookies, chocolate, and milk tea. The N-Gr–N-CNTs/GCE exhibited much larger current responses of the two alkaloids with the most negatively shifted potentials with respect to bare GCE, indicating that the nanocomposite of N-Gr–N-CNTs possessed remarkable electrocatalytic capacity toward the analytes (Jiang, Ding, Jiang, Li, & Mo, 2014). In a later research, a N-CNT-coated GCE was further decorated with poly (L-cysteine) (PLCY) via electropolymerization. Compared to bare GCE, the PLCY/N-CNT/GCE signally increased in the anodic peak currents of theophylline and caffeine from green tea and energy drink by 495.94% and 465.48%, respectively, showing a promoting effect of electrochemical kinetics (Yingzi Wang et al., 2018).

Some polymer surfactants can be coated on carbon-modified electrodes for dispersing and stabilizing carbon nanomaterials, such as cetyltrimethylammonium bromide (CTAB), polymerized 8-aminopyrene-1,3,6-trisulfonic acid [poly(APTA)], and Nafion (Naf). CTAB provides amphiphilic groups that improve peak shape and sensitivity in electroanalytical chemistry, e.g. detecting caffeine in soft drinks by a CTAB–Gr/GCE (J. Y. Sun, Huang, Wei, & Wu, 2011). A nanocomposite of poly(APTA) and single-walled carbon nanotubes (SWCNTs) could form a homogeneous thin film coating on a GCE, boosting the sensitivity of caffeine detection in fruit juices: a relatively high peak current of the caffeine oxidation peak was observed on the poly(APTA)/SWCNTs-GCE, while a SWCNT/GCE and a bare GCE did not reduce the over potential of caffeine oxidation (Sundramoorthy, Sadak, Anandhakumar, & Gunasekaran, 2016). Naf is an antifouling cation exchanger that enriches the analyte cations at the electrode film surface and at the same time prevents direct contact of the substrates with the electrode surfaces. Therefore, it is commonly used to help detect trace amount of alkaloids, most commonly caffeine, in a food matrix, forming nanocomposites on electrodes with MWCNTs (S. Yang et al., 2010; J. Zhang et al., 2011), SWCNTs (Savalia & Chatterjee, 2017), Gr (J. Y. Sun, Huang, Wei, Wu, et al., 2011) , GO (Lezi, Economopoulos, Prodromidis, Economou, & Tagmatarchis, 2017; Zhao et al., 2011), and reduced GO (rGO) (Vasilescu et al., 2015). However, it has been reported that Naf/GCE only outweighs unmodified GCE in analyzing caffeine when the sample mixture contains ascorbate, which reduces the interference from ascorbate with the response at bare electrodes (Carolina Torres, Barsan, & Brett, 2014).

The adhesion between the electrode and the coating material can be enhanced by many biopolymers, *e.g.* poly(folic acid) (PFA) and carboxymethyl cellulose (CMC). Folic acid is an electroactive B-group vitamin, which has been newly developed as a construction agent of electrochemical sensors. For example, a PFA/Gr composite film-modified GCE was successfully used for simultaneous determination of theophylline and caffeine in tea and soft drinks by voltammetry (Shu, Bian, Wang, Qin, & Wang, 2017). CMC is commonly used in food as a viscosity modifier to stabilize emulsions. Its high biocompatibility and hydrophilicity are key promoting factors in a CMC-MWCNTs/GCE detecting trace amount of theobromine from green tea, coffee, and chocolate samples (Peng et al., 2017).

Insert Table 2 here

2.2.2. Metal nanomaterials

Metal nanomaterials, such as cobalt, copper, and gold, are satisfactory candidates to modify electrochemical sensors, due to their large effective surface area, strong adsorption ability, good biocompatibility, and excellent conductivity. It has been reported that $Co(OH)_2$-enfolded Cu_2O nanocubes could be fabricated on an rGO/GCE to detect caffeine in beverages (Velmurugan, Karikalan, Chen, & Karuppiah, 2016). The main reasons of such coating design are: 1) Cu_2O has a distinct shape and grain boundary, making it suitable to prepare nanocubes; 2) cobalt is apt to form shell-like structures, with its redox potential near to caffeine oxidation. In combination, the copper-cobalt bi-metallic system resulted in a two-fold increase of the anodic peak current, giving enhanced detection sensitivity. Similarly, copper sulfide nanoparticles (CuS NPs) have been used to increase the charge transfer capacity of a carbon paste electrode (CPE) in analyzing trace caffeine amount in drinks (Mahanthappa, Yellappa, Kottam, & Srinivasa Rao Vusa, 2016).

Colloidal 24 nm-diameter Au NPs were used to coat on a CPE to determine strychnine in *Strychnos nux-vomica* crude and detoxified seeds, with evidently enhanced catalytic effects compared to a bare electrode. At the bare electrode, strychnine showed a relatively broad and weak oxidation peak; however, the oxidation peak at the Au NPs/CPE was sharp with an intensified (1.955 times) current (Behpour et al., 2011). It was found that Au NPs give better electrocatalytic response when stabilized by chitosan (CHIT), and that synthesizing Au NPs/CHIT nanocomposites in the presence of different organic acids leads to products with different morphology and varied electrochemical performance (Di Carlo et al., 2012). Acetic acid, malonic acid, and oxalic acid have been tested in synthesizing CHIT-stabilized Au NPs; compared to the anodic current recorded on a bare electrode, the increase of current intensity resulting from the three carboxylid acids was 30%, 28%, and 100%, respectively. As a result, the oxalic acid-assisted Au NPs/CHIT-modified electrode presented high performance in detecting caffeine in different drink products (Trani, Petrucci, Marrosu, Zane, & Curulli, 2017). In another study, a conductive polymer (polypyrrole), sol-gel, Au NPs (as an electrochemical active probe), and caffeine were jointly electropolymerized into molecularly

imprinted polymer (MIP) that was used to coat a pencil graphite electrode (PGE). Caffeine was doped during the preparation of MIP/PGE and later removed, leaving the imprinted film with specific binding sites of caffeine molecules in the sol-gel. The ppy/sol-gel/AuNPs layer-by-layer MIP electrode was successfully developed for determining caffeine in green tea, energy, and soda drinks (Rezaei, Khalili Boroujeni, & Ensafi, 2014).

2.3. Nano-fluorophores in fluorescent determination

Wang et al synthesized blue carbon dots (BCD) as fluorophores with L-cysteine, D-(+)-galactose and NaOH for fluorescent determination of caffeine in the soft drink Sprite (T. Y. Wang, Chen, Wang, Tan, & Liao, 2017). In an Inner Filter Effect (IFE) system, the BCD excitation wavelength coincides with the characteristic absorption of caffeine. The consequent irradiation shielding leads to incident light competing and declined fluorescence emission, which is in a linear relationship with the caffeine content.

Zhang et al developed a novel membrane-based flow-through QDs-labeled antibody fluorescence immunoassay (QDs-FLISA) to detect morphine, which was released from poppy shells illegally added to hotpot soup base (C. Zhang et al., 2017). Anti-morphine antibody labeled with CdSe/ZnS QD acted as the fluorescent probe, the intensity of which was negatively proportional to the concentration of morphine.

3. Cyanides

3.1. Fluorescent determination based on Elsner reaction

A unique Elsner reaction can occur between cyanides and some heavy metal atoms, in which cyanides oxidize the metal atoms into ions (Y. Liu et al., 2010). It was originally a hydrometallurgical technique used to extract and purify gold. Later, silver and copper were found to have similar properties to gold (Mahapatra, Datta, & Halder, 2014; Qing et al., 2016). Because of excellent selectivity and easy set-up of the Elsner reaction, researchers have developed gold, silver, and copper nanomaterials for determining trace cyanide in various sample matrices (Table 3).

Gold and copper atoms can be both cyanide reactants and fluorescence probes, which original

fluorescence emission will be “switched off” when the metal atoms are oxidized in reaction with the cyanides. Bovine serum albumin-stabilized gold nanoclusters (BSA-Au NCs) have been applied to determine the amount of cyanide ions in various water samples (Y. Liu et al., 2010). Upon analyte addition, a gold-cyanide complex was formed, accompanied by the disappearance of the original deep brown color and the characteristic emission peak at approximately 640 nm, which were both assigned to the Au NCs. Likewise, copper nanoparticles (Cu NPs) originally showed a blue fluorescence emission at 440 nm, which was quenched upon the addition of cyanides, due to the strong interaction between copper and cyanide in water samples (Momeni, Ahmadi, Safavi, & Nabipour, 2017).

Several “turn-on” fluorescent methods of detecting cyanides in water, milk, plant tissues, and foods were developed by conjugating the gold (Lou et al., 2012; Lou, Zhang, Qin, & Li, 2011; Song, Wu, Wan, & Ma, 2015; Wei, Hsu, Lee, Lin, & Huang, 2012), silver (Mahapatra et al., 2014), and copper (Qing et al., 2016) NPs with other fluoresceins. In these cases, the metal NPs served as both reducing agent and fluorescence quencher in the biosensors. In the absence of cyanides, the fluorescence of the fluoresceins that are attached to the metal MPs is significantly quenched due to the fluorescence resonance energy transfer (FRET) between the metal and the fluorophores. When cyanide ions exist, the metal NP cores will be etched, releasing fluoresceins and turning on the fluorescence emission.

Apart from the heavy metal NPs, other materials have been used as different roles such as sample pre-concentration, gold etching, and fluorescence emission during the determination of cyanides involving Elsner reaction. Dual-functional Au–Fe_3O_4 dumbbell NPs were designed to facilitate sample magnetic purification by the iron oxide magnetic component (Zhai, Jin, Wang, & Dong, 2011). Cerium was used along with gold to prepare BSA-Ce/Au NCs with looser structures compared to those of BSA-Au NCs, facilitating faster accessing and etching of the gold cores by the cyanide ions (C. W. Wang et al., 2016). Graphene-quantum dots (GrQDs) were introduced as fluorescence source with excellent two-photon properties, providing satisfactory two-photon excitation (TPE) signal output when sensing cyanide in complex biological environments (L. Wang et al., 2015).

3.2. Colorimetric determination based on Au NP aggregation

Au NPs have characteristic visible light absorption due to surface plasmon resonance (SPR). There is a red shift in the SPR spectrometry if the Au NPs increase in size or aggregate. An instant red to blue or violet color change, observable by the naked eye would be an indication of Au NP aggregation. As the color change depends on the product concentration, colorimetric sensing enables both quantitative and qualitative analyses of gold-reactive substances (Nilam, Hennig, Nau, & Assaf, 2017).

Liu et al utilized this property of Au NPs to detect cyanide and linamarin, a cyanide glycoside, in cassava roots, peach kernels, and loquat kernels (C.-Y. Liu & Tseng, 2011, 2012). A neutral surfactant, PS 40, was used to stabilize citrate-capped Au NPs in a high-salt environment, resulting in a pink solution. Cyanide or linamarin detached the Au NPs from PS 40 by forming AuCN precipitates and/or $Au(CN)^{2-}$ ions; the Au NPs therefore assembled and presented a violet color. The PS 40-Au NP probe was used to monitor the removal of cyanide during food processing and quantify the amount of total cyanide in the food samples.

Castro et al employed the theory of Au NP aggregation from another angle, using the fact that copper diethyldithiocarbamate [$Cu(DDTC)_2$] takes precedence over adenosine triphosphate (ATP)-stabilized Au NPs in reacting with cyanide. Once the $Cu(DDTC)_2$-complex reacted with cyanide, the free DDTC caused Au NP aggregation, indicating the cyanide content in samples (González-Castro, Peña-Vázquez, & Bermejo-Barrera, 2015).

3.3. Other determination methods

An electrochemical enzyme inhibition biosensor was developed based on a CHIT-horseradish peroxidase (HRP)/hydroxyapatite nanowire array (HANWA)/GCE. The HANWA coated the electrode and provided large surface area and abundant adsorbing sites for HRP-cyanide interaction. A reduced electrochemical response could be measured as the cyanide content increased in distilled wine and edible cassava starch (S. Wang et al., 2010). Cyanamides from 21 plant-derived foods were determined by LC-MS/MS preceded by clean-up with MWCNTs and derivatization with

dansyl chloride (Cheng et al., 2018). In the study, MWCNTs exhibited good purification by adsorbing the interference substances in complex matrices.

Insert Table 3 here

4. Proteins and corresponding DNAs

4.1. Electrochemical determination: antibody, aptamer, and DNA as target probes

Electrochemical determination of proteins and DNAs usually involves enzymatic oxido-reduction. The electrochemical signal from such oxido-reduction can be detected quantitatively, either in positive or negative correlation with analyte concentration. When antibodies are used as protein probes, nanomaterials are often used to coat the electrodes, not only improving electrochemical response but also engaging in target-probe interaction (Table 4). Alves et al have developed a voltammetric biosensor consisting of Au NP-coated screen-printed carbon electrode (SPCE) combined with sandwich immunoassay to detect peanut allergens Ara h 1 and Ara h 6 in food samples (Alves, Pimentel, Nouws, Correr, et al., 2015; Alves, Pimentel, Nouws, Marques, et al., 2015). The Au NPs were conjugated with monoclonal antibodies capturing the analyte proteins; detection antibodies labeled with alkaline phosphate (AP) consequently bound with the immobilized allergens. The enzymatic reaction was carried out in a substrate solution containing 3-indoxyl phosphate (3-IP) and silver nitrate. The AP-hydrolyzed intermediate of 3-IP reduced the silver ions to metallic silver. The electrochemical stripping current of the enzymatically deposited silver was recorded in a linear sweep voltammagram, positively corresponding to the peanut allergen amount in the food samples (Fig. 1A).

The protein-antibody electrochemical reaction system can also be designed to generate signals that negatively correlate with analyte content. A competitive immunosensor based on an Au NP-modified SPCE was fabricated to detect gliadin in food samples made of different flours (Manfredi et al., 2016). Gliadin molecules were immobilized to the Au NPs/SPCE beforehand. A mixture of AP-labeled anti-gliadin antibodies, free gliadin from a sample, and hydroquinone diphosphate (HQDP) was transferred to the working electrode. The free and immobilized gliadin molecules competed with each other to bind to the AP-conjugated antibodies. The higher the

concentration of free gliadin in a sample, the less enzyme-linked antibody could be bound to the immunosensor surface. AP promoted dephosphorylation of HQDP, yielding electroactive hydroquinone (HQ), which was subsequently oxidized into quinone (Q) during the differential pulse voltammetry (DPV) scan, ultimately presenting the gliadin-related analytical signal (Fig. 1B). Another reverse-signaling of gliadin from foods was conducted by a GCE, which was functionalized with anti-gliadin antibody-linked porous reduced graphene oxide (prGO) (Chekin et al., 2016). $[Fe(CN)_6]^{3-/4-}$ was used as a redox probe; the generated current was reduced by the presence of gliadin from samples. The porous electrode coating shows advantages in electrochemical sensing material for two reasons: 1) its huge surface area allows immobilization of a high number of ligands, increasing the detection sensitivity (limit of detection, LOD, 1.2 ng/mL), and 2) its interconnected pores promote diffusion of the analyte, facilitating fast sensing.

Insert Table 4 here

Insert Fig. 1 here

Aptamers are effective protein receptors with sizes at the nano-level. A competitive aptaassay has been reported to detect gliadin from food matrixes via aptamer-target binding. A 80-nt aptamer with the highest affinity to 33-mer, an immunodominant apolar peptide from α2-gliadin, was selected from a library of DNA oligonucleotides by a Systematic Evolution of Ligands by EXponential enrichment (SELEX) method (Lamont, He, Warriner, Labuza, & Sreevatsan, 2011; Tuerk & Gold, 1990). Magnetic particles capped with 33-mer and streptavidin-peroxidase conjugate (strep-MP) were involved in the assay. A strep-HRP substrate, 3,3′,5,5′-tetramethylbenzidine (TMB), was added to the system to generate oxido-reduction current to be chromoamperametrically recorded. In the presence of a fixed amount of the selected aptamer, competition existed between the immobilized peptide on the strep-MP and gliadin from the sample solution. When the gliadin concentration in the sample increased, the amount of free aptamer available to bind 33-mer on the MPs surface diminished, resulting in a decreasing analytical signal (Amaya-González, De-Los-Santos-Álvarez, Miranda-Ordieres, & Lobo-Castañón, 2014). Unlike the abovementioned electrochemical protein detection methods relying on redox reactions, an enzyme-free detection of ricin was achieved by White et al through assembling a delicate floating gate electrode (FGE) with a DNA aptamer to

capture the analyte. A poly(3-hexylthiophene) (P3HT) semiconductor channel and a control gate (CG) was designed on the left and right side of the FGE, respectively. When ricin bound to the aptamer-functionalized FGE, the PEHT conductivity changed, resulting in an abrupt shift of trip voltage (VT) at the CG, which was constantly monitored. The voltage change was in positive correlation with ricin concentration. The measurement was fast (in minutes) since no preprocessing, enzymatic reaction, or rinsing steps were needed (White, Sreevatsan, Frisbie, & Dorfman, 2016).

Stem-loop DNA probes have been developed to monitor target genes of toxin proteins. When a target DNA is captured, the stem-loop structure of the probe undergoes a conformational change. The hybridization process alters electron-transfer efficiency, allowing the electrochemical signal to be monitored for quantitative assay. Sun et al managed to use multilayer Gr–Au NP nanocomposites to modify DNA probes for detection of Ara h 1 in peanut milk; the nanomaterials evidently amplified the electrochemical signals (LOD 0.041 fM) (X. Sun, Jia, Guan, et al., 2015). The same team made another DNA biosensor for Ara h 1 in peanuts with CHIT–MWCNTs deposited on a GCE, which could immobilize the DNA probes and promote electron transfer kinetics (X. Sun, Jia, Ji, et al., 2015). Strep-HRP and biotin were conjugated on the top of the probes for signal amplification. The conformational change of the probe upon target recognition triggered specific biotin-SA-HRP interactions on the electrode surface, generating electrochemical signals that could be used to quantify the target content.

4.2. Surface-enhanced Raman scattering determination: nanomaterials as system conjugators and signal amplifiers

Gold, silica, and silver nanomaterials have been playing important roles as conjugators in the SERS sensing system to detect trace amount of toxic plant-derived proteins in foods. Szlag and coworkers used silica nanospheres (Si NSs) and 80 nm of gold film-over-nanospheres (Au FONs) to construct a SERS platform for the attachment of poly N-acetyl-galactos-amine ethyl methacrylamide (NAGEMA), a glycopolymer which can recognize ricin B-chain (RBC) (Szlag et al., 2016). The conjugated biosensor was proved effective in detecting spiked ricin in apple and orange juices. Tang et al optimized single-stranded oligodeoxynucleotides (ssODNs) named poly(21dA), and attached the sequence to Au NPs to give ssODN−AuNPs as the detector complex (Tang et al., 2016). The

ssODN−AuNPs were anchored on a modified Si wafer, forming a mechanically stable SERS chip. Active ricin specifically depurinated the poly(21dA) sequences and released adenines from the sensing interface, leading to distinctive SERS signal attenuation based on the fingerprint of adenine. A sandwich RBC-sensing system composed of Si substrate–poly (N-Acryoyl-L-valine)–RBC aptamer (to immobilize RBC from sample matrix) and RBC aptamer–Ag NP–4,40-bipyridyl (Bpy) (to work as SERS probe) was established to detect ricin in artificially contaminated orange juice and milk (Zengin, Tamer, & Caykara, 2015). Being the core of the SERS probe, the Ag NPs were dual-labeled with aptamer and Bpy, the Raman reporter. Another silver-containing SERS detection platform has been reported employing aptamer-conjugated silver dendrites to capture ricin from liquid foods; the SERS spectrum of the captured target can be observed consequently. The silver dendrites were composed of Ag NPs of 50 nm in diameter (He, Lamont, et al., 2011).

Rough metallic particles, such as Au NPs and Ag NPs, are usually adopted as SERS signal amplifiers, since they have strong enhancing effect on local light fields (Staiano et al., 2009). In a fiber optic surface plasmon resonance (FO-SPR) biosensor for detecting Ara h 1 protein in a candy bar, Au NPs were involved in the sandwich bioassay to amplify the final signal; they increased the sensitivity to a LOD of 75 nM (Tran et al., 2013). The captured target protein was recognized by a specific antibody, the Fc region of which had a high affinity for a bacterial protein that is linked to the Au NPs. Silver nanoshell (Tang et al., 2016), dendrite (He, Deen, et al., 2011), and particle deposition (Zengin et al., 2015) are popular agents used to coat on the sensing complex surface to enhance SERS response to different degrees (Table 4).

4.3. Fluorescent determination: nanomaterials as response adjustors

4.3.1. Fluorescence sources

CdSe/ZnS core-shell QDs have often been adopted as fluorescence sources, sometimes covalently bound with specific antibodies for selective analyte determination. Ansari et al tagged the QDs with anti-gliadin antibodies to identify the changes in the distribution of gliadin during bread baking in comparison to dough (Ansari et al., 2015). Sections of bread samples were mounted on glass slides, topped by a solution of QD-antibody conjugates. The QDs were then visualized in 3D by a confocal laser scanning microscope, revealing that the distribution of gliadin proteins largely depended on

baking time and the location of layers in flat bread. QDs were also conjugated with Ara h 1 gene-binding aptamer for the integration of a “turn on” microfluidic chip to detect peanut allergens in biscuit samples (Weng & Neethirajan, 2016).

However, conventional fluorescent bioprobes of QDs have drawbacks including photobleaching of organic dyes and interference of background autofluorescence. In light of this, lanthanide-doped inorganic NPs have emerged as a promising new class of fluorophore. For example, amine-functional europium-doped $KGdF_4$ NPs have been linked to ricin aptamers as probes for the toxic protein. The transient decay of the $KGdF_4:Eu^{3+}$ NPs has been recorded as time-resolved fluorescence (TR-FL) signals (Huang et al., 2015). Such TR-FL NPs have large effective Stock shifts (more than 300 nm), avoiding IFE due to fluorophore excitation and emission spectra overlap. These novel probes also have much longer fluorescence lifetime (on the order of milliseconds) than those of QDs (on the order of nanoseconds or microseconds), eliminating interference of biological matrix emission and complex sample autofluorescence based on TR-FL determination (Eliseeva & Bünzli, 2010).

4.3.2. Quenching agents

It is reported that carbon nanomaterials, especially GO, are effective energy acceptor and have delocalized electronic excitations, enabling long-range resonance energy transfer (LrRET). Thus they can quench the emission of fluorophore efficiently (Y. Zhang, Liu, Zhen, & Huang, 2011). In an abovementioned study of detecting ricin in a sample mixture by $KGdF_4:Eu^{3+}$ NPs, GO was used as a competitor of ricin to adsorb the aptamer and a quencher of the excited donor fluorophore (Huang et al., 2015). The aptamer converted to a rigid tertiary structure when recognizing the ricin molecule. Thus, it could not be bound and quenched by GO, giving rise to partial fluorescence in proportion to the target amount. The conformational change of a DNA-binding aptamer has also been utilized to detect Ara h 1 gene in food samples. It was found that QD-aptamer-GO changed in shape upon interaction with the food allergens, resulting in fluorescence difference due to quenching and recovering signal by GO (Weng & Neethirajan, 2016).

Li et al developed a strand displacement amplification platform for ricin detection in orange juice

and caster beans using GO as a quencher and RBC-binding aptamer as recognition element (C. H. Li et al., 2017). The aptamer was originally hybridized with a short blocker nucleotide sequence, which would be replaced by RBC. The released blocker then opened and hybridized with a carboxytetramethylrhodamine (TAMRA, a fluorophore)-modified hairpin ssDNA probe. The hairpin triggered an isothermal strand-displacement polymerase reaction (ISDPR) and resulted in a large amount of TAMRA-labeled duplex DNAs that could not bound to nor be quenched by GO due to shielding of nucleobases, leading to strong fluorescence intensity. In contrast, in the absence of ricin, the stem-loop hairpin structure could easily be adsorbed on the GO surface through π-π stacking and non-covalent hydrophobic interactions, strongly quenching the TAMRA fluorescence. Therefore, RBC could be sensitively detected (LOD 0.6 μg/mL) by the significantly increased fluorescence intensity (Fig. 1C).

The quenching effect of GO can be avoided by maintaining distance between GO and the fluorophore. To achieve such effect, a fluorophore-modified DNA probe was hybridized first with a capture ssDNA with an A_{20} tail. The exposed A_{20} nucleobases interacted with GO surface, leaving the hybridized portion of the probe and capture DNA "standing" on GO, keeping the fluorescent source away from the quencher. The method was proved successful in improving detection sensitivity (LOD 400 ng/mL) in quantifying spiked RBC in orange juice (Xiao, Tao, Zhang, Huang, & Zhen, 2016) (Fig. 1D).

4.3.3. Signal amplifiers

GO is not only an effective fluorescence quencher, but also an excellent fluorescence anisotropy (FA) amplifier. Different from intensity signals, FA is an intrinsic parameter, which ultimately relates to the observed polarization on the rotational diffusion rate of molecules (Jameson, 2011). Compared to zero-dimensional (0D) spherical NPs with the same surface area, GO has a unique 2D nanosheet structure and a larger mass, together resulting in slower rotation rate than that of NPs; thus it can amplify the FA signal of the analyte (Xiao, Li, Huang, & Zhen, 2015).

An exonuclease III (Exo III)-aided GO-amplified FA sensing system using aptamer as recognition element was established to detect RBC in drink samples (Xiao et al., 2016). The TAMRA-modified

DNA probe with an A_{20} tail was anchored on the GO surface; the nucleotide tail not only maintained distance between GO and TAMRA, decreasing the fluorescence quenching effect but also it facilitated the rotation of the dye coupled with the entire formation to obtain high FA. The RBC-binding aptamer was hybridized with a short blocker sequence, which was released upon addition of ricin. The free blocker subsequently hybridized with the DNA probe and detached the probe from the GO surface via toehold-mediated strand exchange reaction, largely reducing the FA signal. Furthermore, the Exo III digested the probe DNA from the probe-blocker duplex into small fragments of decreased molecular mass with even lower FA. The blocker, freed from the duplex, then reacted with another probe DNA on GO surface and initiated the next round of cleavage, achieving Exo III-catalyzed target recycling signal amplification. Eventually, RBC could be sensitively detected by the substantially decreased FA (Fig. 1D).

Ag NPs have long known to have impressive fluorescence enhancement for two major reasons: 1) local field enhancement and 2) radiative decay engineering. The second cause leads to interaction of excited molecules with the Ag NPs, increasing the molecules' brightness and decreasing their lifetimes. An enhanced fluorescence emission on silver island films (SIFS) with the total internal reflection fluorescence mode (TIRF) was developed as a new assay format to detect gliadin in flour samples (Staiano et al., 2009). SIFs conjugated with anti-gliadin antibodies were coated on glass slides; the antigen from the sample was captured and further covered by fluorophore-labeled detection antibodies. The ultimate signal was detected by TIRF. A 5-fold improvement of the signal from SIFs, and was observed compared to bare glass slides without silver coating, indicating the strong fluorescence enhancement due to the silver nanomaterials.

Apart from carbon and metals, organic nanomaterials have also been proved capable of enhancing fluorescence signals. Chu et al incorporated anti-gliadin antibody-conjugated immunomagnetic beads (IMBs) and fluorescent dyes-loaded immunoliposomal nanovesicles (IMLNs) into a sandwich complex of IMBs–gliadin–IMLNs, to check for gluten contamination in raw materials and in gluten-free foods (Chu & Wen, 2013). The IMLNs was synthesized with dipalmitoyl phosphatidylcholine (DPPC), dipalmitoyl phosphatidylglycerol (DPPG), dipalmitoyl phosphatidylethanolamine (DPPE), N-succinimidyl-S-acetylthiopropionate (SATA), cholesterol,

and chloroform. Closed spherical vesicles of IMLNS consisted of one or more phospholipid bilayers surrounding an aqueous cavity. The hollow sphere encapsulated a huge amount of fluorescent dye molecules, releasing of which immediately and significantly intensified the assay signal (with an LOD of 0.6 μg/mL).

5. Multifunctional nanomaterials as detecting tools

Nanomaterials taking part in phytotoxin detection mainly have four roles: 1) sample pretreatment; 2) sensor structure mediation, 3) target recognition or reaction; and 4) signaling (Fig. 2). Sample pretreatment is usually achieved by carbon and iron oxide-based materials, either enriching the analyte or eliminating foreign substances. Carbon, silica, and metals often serve as components of the sensory platform, either providing structural support, *e.g.* by linking an antibody with a signaling probe, or improving detection sensitivity or selectivity, *e.g.* by electrode surface modification. Recognizing the target is achieved either by molecular probes, most commonly antibodies and aptamers, or by target-characteristic reactions, such as the Elsner reaction of cyanides with gold, silver, and copper. Target signaling can be conducted by nanomaterials being the fluorescence/color source or altering spectrometric signals.

Insert Fig. 2 here

5.1. Carbon nanotubes

In the determination of trace analyte from a complex mixture, both MWCNTs and SWCNTs have played multiple roles in various circumstances, such as effective SPE adsorbents, electrode surface modifiers, and the electrode itself. With large surface area and unique structure, MWCNTs can attract oxygen-containing chemicals by strong hydrophobic and ionic interactions. Adsorbing properties can be utilized in sample pre-concentration or matrix clean-up, depending on the nature of the analytes. Carbon material has been adopted to enrich caffeine content prior to fluorescent detection (Talio et al., 2014), as well as to eliminate organic impurities in cyanide detection before LC-MS/MS analysis (Cheng et al., 2018). Moreover, MWCNTs have frequently been coated on carbon electrodes to enhance selectivity and sensitivity of electrochemical determination of small molecules, especially alkaloids reducing the LOD to the order of μM (Behpour et al., 2012; Gupta,

Jain, & Shoora, 2013). They can also directly function as electrodes; some of such electrodes are covalently bound with polymer surfactants to enhance the determination performance, *e.g.* better peak shape, higher detection sensitivity, and longer biosensor operational life span (Dar et al., 2012).

Similarly, SWCNTs often participate in electrochemical analysis with electrode-related functions. They can help achieve simultaneous determination of multiple alkaloids on an electrode, e.g. carbon-ceramic electrode (Habibi, Abazari, & Pournaghi-Azar, 2014). DNA-functionalized SWCNT can be stabilized on an electrode by Naf due to the excellent film forming ability of the surfactant; a Naf/DNA-SWCNT/GCE can remarkably enhance the electro-oxidation signal (7.8 fold higher than that of bare GCE) of alkaloid analytes in complex mixtures (Yanwei Wang, Wei, Wang, & Li, 2014). Moreover, a DNA-modified SWCNT paste electrode exerts a more sensitive detection of caffeine from plant tissues (LOD 0.35 μM) than an ordinary CPE does (LOD 51.2 μM) (Ly, Lee, & Jung, 2009).

5.2. Graphene oxide

Like other carbon-based nanomaterials, GO is an ideal adsorbing agent due to its outstanding surface area and large quantities of oxygen on the surface, which enables interactions with organic compounds containing oxygen- and nitrogen-containing functional groups. For instance, studies have been carried out to apply GO as capillary interior coating (J. Li, Ye, Gao, Zhou, & Ma, 2015) or SPE sorbent (Sereshti et al., 2014) to detect alkaloids.

Structure refinement of GO has been explored to increase the sensitivity of analyte determination. GO prepared by different methods may vary in oxygen content, leading to different analytical performance. GO functionalized with Naf has been used for electrode surface modification for alkaloid determination (Zhao et al., 2011). rGO can be obtained by electrochemically reducing GO, with much lower number of oxygen atoms on the surface. rGO possess advantages over GO in electrochemical sensing with increased active area and facilitated mass transport (Ambrosi et al., 2016). rGO has been utilized directly as an electrode (Khoo, Pumera, & Bonanni, 2013) or as an electrode coating in combination with metal components (Velmurugan et al., 2016). prGO further

outweighs rGO with its increased surface area due to porosity; it can considerably increase the redox current generated from the electrochemical sensor (Chekin et al., 2016). prGO has been deposited on an electrode surface to anchor antibodies that specifically recognize target proteins, for allergen determination (Chekin et al., 2016).

In addition to functioning as sorbent and electrochemical sensing mediator, GO also affects signal intensity in fluorescent analyses. It is an efficient fluorophore quencher with excellent energy accepting capability (Huang et al., 2015). It is also an FA signal amplifier due to its 2D nanosheet structure and relatively high surface density, *i.e.* mass per unit area (Xiao et al., 2016). The GO properties of signal suppression or enhancement have been extensively utilized in determining proteins or DNAs in complex samples with "turn on" or "switch off" fluorescent systems.

5.3. Gold nanoparticles

Au NPs are highly multifunctional due to their exclusive physical and chemical properties. They are heavily involved in the sensitive detection of small and large biomolecules, playing different roles as structural mediator, target reactant, or signal adjustor. It is highly possible that the diverse capacities of Au NPs can be integrated, making the nanomaterial into a powerful agent that can simultaneously participate in different phases of chemical detections.

Au NPs have relatively low requirements for conjugating with other substances, thus metal particles are frequently utilized to link different sensory parts within a biosensor. Au NPs can be coated on an electrode and subsequently capped with antibodies to immobilize and detect target proteins. For example, such surface modification of an electrode contributed to increased antibody binding sites and subsequent target mass on a quartz crystal microbalance (QCM) chip. In an analysis of different cereals and commercial food products, the modified electrode showed 48% greater target recognition than the bare one (Chu, Lin, Chen, Chen, & Wen, 2012). In another Au NP-based protein analysis, Au NPs were dually bound with antibodies and barcode DNAs. The antibodies specifically recognized the target; the barcode DNAs annealed to signaling DNAs. The signaling DNA sequences were quantified by a real-time PCR method, reflecting target concentration in the samples (H. Q. Yin, Jia, Yang, Wang, & Zhang, 2012).

Au NPs can contribute as reducing agents in sensitive detection of cyanide via the unique Elsner reaction between cyanides and gold atoms. Various fluorescent sensor components, such as stabilizers and fluoresceins, can be employed with the reaction in sensing cyanide in complex samples (Qing et al., 2016).

The aggregation of gold atoms induces a visible change of color, which makes the gold particles convenient sensing agents (Nilam et al., 2017). Interestingly, Au NPs also possess peroxidase-like ability to catalyze TMB, resulting in a color change in the solution. The catalytic capability of Au NPs can be improved or reduced by binding to or desorbing from a target-specific aptamer. Such property of the particles was successfully utilized to detect spiked abrin in milk (Hu et al., 2015). Moreover, Au NP accepts energy efficiently and therefore is able to quench fluorophores and lead to a decrease in fluorescence intensity (Song et al., 2015). Furthermore, it has been discovered that the gold particles can amplify the SERS signal, and thus they can also be employed for sensitive molecule determination.

6. Conclusion and outlook

This review summarizes recent progress in nanomaterial-based determination of food phytotoxins, including alkaloids, cyanides, and proteins. Analyte-specific sensing strategies are mainly employed to suit physical or chemical properties of the target molecules. Electrochemistry is a suitable technique to detect alkaloids, since the analyte redox current can be proportional to the concentration under optimized conditions. Fluorescent and colorimetric analyses are frequently adopted for cyano-compounds, since cyanides can undergo the unique Elsner reaction with some heavy metal atoms. Detection of biomacromolecules like proteins and their corresponding DNAs involves specific recognition by antibodies or aptamers hyphenated with various detection methods. During the above determination processes, nanomaterials mainly take part in four phases: sample pretreatment, sensor structure mediation, target recognition and reaction, and signaling. Some nanomaterials are capable of playing more than one of the above roles; their multifunctionality hints at great potential to be developed into upgraded biosensors for toxic phytocomponents in foods.

Great achievements have been made in the detection of trace plant-derived toxins in food matrices, yet there are still challenges awaiting further investigation. Up till now, only a few alkaloids can be detected in food samples by nanomaterial-assisted electrochemical analysis because oxidation peaks of structurally similar chemicals may overlap, giving false positive signals. Approaches to further enhance detection selectivity of the working electrodes are to be explored to evaluate other commonly found toxic phytoalkaloids, such as pyrrolizidine alkaloids that exist in a wide range of plant species. One possible solution may be exploring categories of nanomaterials other than carbon and considering metal surface modification on electrodes. The current detection of proteins has been mainly based on specific antigen-antibody or analyte-nucleotide sequence recognition, with the result that only one protein can be screened at a time. Miniaturization would allow multiple elements to be recognized simultaneously, e.g. via high-throughput screening of different targets. Another direction of research in this field is commercialization of nanosensors determining endogenous hazardous components from plant-derived foods. By commercializing the research into practical procedures for food quality control can be of benefit to the public.

Acknowledgment

This work was partially supported by the National Natural Science Foundation of China (81673691), the Applied Basic Research Program of Sichuan Province (2018JY0445), the Innovation and Technology Fund of Hong Kong (ITS/280/15), the Guangdong Natural Science Foundation (2014A030313766), and the Shenzhen Science and Technology Innovation Committee (JCYJ20160518094706544).

References

Agency for Toxic Substances and Disease Registry. (1989). *Toxicological profile for cyanide*. Agency for Toxic Substances and Disease Registry, Syracuse Research Corporation.

Alves, R. C., Pimentel, F. B., Nouws, H. P. A., Correr, W., González-García, M. B., Oliveira, M. B. P. P., & Delerue-Matos, C. (2015). Detection of the peanut allergen Ara h 6 in foodstuffs using a voltammetric biosensing approach. *Analytical and Bioanalytical Chemistry*, *407*(23), 7157–7163.

Alves, R. C., Pimentel, F. B., Nouws, H. P. A., Marques, R. C. B., González-García, M. B., Oliveira, M. B. P. P., & Delerue-Matos, C. (2015). Detection of Ara h 1 (a major peanut allergen) in food using an electrochemical gold nanoparticle-coated screen-printed immunosensor.

Biosensors and Bioelectronics, *64*, 19–24.

Amaya-González, S., De-Los-Santos-Álvarez, N., Miranda-Ordieres, A. J., & Lobo-Castañón, M. J. (2014). Aptamer binding to celiac disease-triggering hydrophobic proteins: A sensitive gluten detection approach. *Analytical Chemistry*, *86*(5), 2733–2739.

Ambrosi, A., Chua, C. K., Latiff, N. M., Loo, A. H., Wong, C. H. A., Eng, A. Y. S., … Pumera, M. (2016). Graphene and its electrochemistry-an update. *Chem. Soc. Rev.*, *45*(9), 2458–2493.

Ansari, S., Bozkurt, F., Yazar, G., Ryan, V., Bhunia, A., & Kokini, J. (2015). Probing the distribution of gliadin proteins in dough and baked bread using conjugated quantum dots as a labeling tool. *Journal of Cereal Science*, *63*, 41–48.

Ariga, K., Vinu, A., Miyahara, M., Hill, J. P., & Mori, T. (2007). One-pot separation of tea components through selective adsorption on pore-engineered nanocarbon, carbon nanocage. *Journal of the American Chemical Society*, *129*(36), 11022–11023.

Augusto, F., Hantao, L. W., Mogollón, N. G. S., & Braga, S. C. G. N. (2013). New materials and trends in sorbents for solid-phase extraction. *TrAC - Trends in Analytical Chemistry*, *43*(x), 14–23.

Bahrani, S., Ghaedi, M., Dashtian, K., Ostovan, A., Mansoorkhani, M. J. K., & Salehi, A. (2017). MOF-5(Zn)-Fe2O4 nanocomposite based magnetic solid-phase microextraction followed by HPLC-UV for efficient enrichment of colchicine in root of colchicium extracts and plasma samples. *Journal of Chromatography B: Analytical Technologies in the Biomedical and Life Sciences*, *1067*, 45–52.

Behpour, M., Ghoreishi, S. M., Khayatkashani, M., & Motaghedifar, M. (2011). Determination of strychnine in *Strychnos nux-vomica* crude and detoxified seeds by voltammetric method using a carbon paste electrode incorporated with gold nanoparticles. *Analytical Methods*, *3*(4), 872–876.

Behpour, M., Ghoreishi, S. M., Khayatkashani, M., & Motaghedifard, M. (2012). A new method for the simultaneous analysis of strychnine and brucine in *Strychnos nux-vomica* unprocessed and processed seeds using a carbon-paste electrode modified with multi-walled carbon nanotubes. *Phytochemical Analysis*, *23*(2), 95–102.

Carolina Torres, A., Barsan, M. M., & Brett, C. M. A. (2014). Simple electrochemical sensor for caffeine based on carbon and Nafion-modified carbon electrodes. *Food Chemistry*, (149), 215–220.

Chai, C., Lee, J., & Takhistov, P. (2010). Direct detection of the biological toxin in acidic environment by electrochemical impedimetric immunosensor. *Sensors (Switzerland)*, *10*(12), 11414–11427.

Chekin, F., Singh, S. K., Vasilescu, A., Dhavale, V. M., Kurungot, S., Boukherroub, R., & Szunerits, S. (2016). Reduced graphene oxide modified electrodes for sensitive sensing of gliadin in food samples. *ACS Sensors*, *1*(12), 1462–1470.

Cheng, C., Di, S., Zhang, W., Chen, L., Tian, Z., Zhou, Z., & Diao, J. (2018). Determination of cyanamide residue in 21 plant-derived foods by liquid chromatography-tandem mass

spectrometry. *Food Chemistry*, *239*, 529–534.

Chu, P. T., Lin, C. S., Chen, W. J., Chen, C. F., & Wen, H. W. (2012). Detection of gliadin in foods using a quartz crystal microbalance biosensor that incorporates gold nanoparticles. *Journal of Agricultural and Food Chemistry*, *60*(26), 6483–6492.

Chu, P. T., & Wen, H. W. (2013). Sensitive detection and quantification of gliadin contamination in gluten-free food with immunomagnetic beads based liposomal fluorescence immunoassay. *Analytica Chimica Acta*, *787*, 246–253.

Dar, R. A., Brahman, P. K., Tiwari, S., & Pitre, K. S. (2012). Electrochemical determination of atropine at multi-wall carbon nanotube electrode based on the enhancement effect of sodium dodecyl benzene sulfonate. *Colloids and Surfaces B: Biointerfaces*, *91*(Supplement C), 10–17.

Di Carlo, G., Curulli, A., Toro, R. G., Bianchini, C., De Caro, T., Padeletti, G., … Ingo, G. M. (2012). Green synthesis of gold–chitosan nanocomposites for caffeic acid sensing. *Langmuir*, *28*(12), 5471–5479.

Eliseeva, S. V., & Bünzli, J.-C. G. (2010). Lanthanide luminescence for functional materials and bio-sciences. *Chem. Soc. Rev.*, *39*(1), 189–227.

European Food Safety Authority. (2008). Ricin (from Ricinus communis) as undesirable substances in animal feed - Scientific Opinion of the Panel on Contaminants in the Food Chain. *EFSA Journal*, *6*(9), 726.

Feng, Z. F., Xu, Y. H., Wei, S. G., Zhang, B., Guan, F. L., & Li, S. B. (2015). Fabrication of Fe3O4 nanoparticle-coalesced hydroxylated multi-walled carbon nanotubes for the analysis of strychnine in human serum.

Filik, H., & Aslıhan Avan, A. (2018). Conducting polymer modified screen-printed carbon electrode coupled with magnetic solid phase microextraction for determination of caffeine. *Food Chemistry*, *242*, 301–307.

Gaudin, C., Cunha, D., Ivanoff, E., Horcajada, P., Chevé, G., Yasri, A., … Maurin, G. (2012). A quantitative structure activity relationship approach to probe the influence of the functionalization on the drug encapsulation of porous metal-organic frameworks. *Microporous and Mesoporous Materials*, *157*, 124–130.

Ghosh, K., Kumar, M., Maruyama, T., & Ando, Y. (2010). Tailoring the field emission property of nitrogen-doped carbon nanotubes by controlling the graphitic/pyridinic substitution. *Carbon*, *48*(1), 191–200.

Gleason, M. N., Gosselin, R. E., & Hodge, H. C. (1957). Clinical toxicology of commercial products. *Baltimore: The Williams and Wilkins Company*, 174.

González-Castro, A., Peña-Vázquez, E., & Bermejo-Barrera, P. (2015). A fast and simple method to perform cyanide detection using ATP stabilized gold nanoparticles combined with the Cu(DDTC)2 complex. *Anal. Methods*, *7*(10), 4308–4314.

Gupta, V. K., Jain, A. K., & Shoora, S. K. (2013). Multiwall carbon nanotube modified glassy carbon electrode as voltammetric sensor for the simultaneous determination of ascorbic acid and caffeine. *Electrochimica Acta*, *93*, 248–253.

Habibi, B., Abazari, M., & Pournaghi-Azar, M. H. (2014). Simultaneous determination of codeine and caffeine using single-walled carbon nanotubes modified carbon-ceramic electrode. *Colloids and Surfaces B: Biointerfaces*, *114*, 89–95.

He, L., Deen, B., Rodda, T., Ronningen, I., Blasius, T., Haynes, C., … Labuza, T. P. (2011). Rapid detection of ricin in milk using immunomagnetic separation combined with surface-enhanced raman spectroscopy. *Journal of Food Science*, *76*(5), N49–N53.

He, L., Lamont, E., Veeregowda, B., Sreevatsan, S., Haynes, C. L., Diez-Gonzalez, F., & Labuza, T. P. (2011). Aptamer-based surface-enhanced Raman scattering detection of ricin in liquid foods. *Chemical Science*, *2*(8), 1579–1582.

Hennion, M. (1999). Solid-phase extraction: method development, sorbents, and coupling with liquid chromatography. *Journal of Chromatography A*, *856*, 3–54.

Hensperger, B. (2001). *Bread for Breakfast*. Emeryville: Ten Speed Press.

Hirayama, I., Hiruma, T., Ueda, Y., Doi, K., & Morimura, N. (2018). A critically ill patient after a colchicine overdose below the lethal dose: a case report. *Journal of Medical Case Reports*, *12*(1), 191–195.

Hu, J., Ni, P., Dai, H., Sun, Y., Wang, Y., Jiang, S., & Li, Z. (2015). Aptamer-based colorimetric biosensing of abrin using catalytic gold nanoparticles. *Analyst*, *140*(10), 3581–3586.

Huang, Y., Chen, X., Wu, S., Duan, N., Yu, Y., & Wang, Z. (2015). Homogeneous time-resolved fluorescence assay for the detection of ricin using an aptamer immobilized on europium-doped KGdF4 nanoparticles and graphene oxide as a quencher. *Microchimica Acta*, *182*(5–6), 1035–1043.

Jameson, D. M. (2011). Fluorescence polarisation/anisotropy in diagnostics and imaging. *Burns*, *110*(5), 2685–2708.

Jiang, L., Ding, Y., Jiang, F., Li, L., & Mo, F. (2014). Electrodeposited nitrogen-doped graphene/carbon nanotubes nanocomposite as enhancer for simultaneous and sensitive voltammetric determination of caffeine and vanillin. *Analytica Chimica Acta*, *833*, 22–28.

Johnson, R. C., Zhou, Y., Jain, R., Lemire, S. W., Fox, S., Sabourin, P., & Barr, J. R. (2009). Quantification of l-abrine in human and rat urine: A biomarker for the toxin abrin. *Journal of Analytical Toxicology*, *33*(2), 77–84.

Khoo, W. Y. H., Pumera, M., & Bonanni, A. (2013). Graphene platforms for the detection of caffeine in real samples. *Analytica Chimica Acta*, *804*, 92–97.

Knutsen, H. K., Alexander, J., Barregård, L., Bignami, M., Brüschweiler, B., Ceccatelli, S., … Vleminckx, C. (2018). Update of the Scientific Opinion on opium alkaloids in poppy seeds. *EFSA Journal*, *16*(5), 5243–5361.

Lamont, E. A., He, L., Warriner, K., Labuza, T. P., & Sreevatsan, S. (2011). A single DNA aptamer functions as a biosensor for ricin. *The Analyst*, *136*(19), 3884.

Lewis, R. J., & Sax, N. (2004). *Sax's dangerous properties of industrial materials* (11th ed.). Hoboken: Wiley-Interscience.

Lezi, N., Economopoulos, S., Prodromidis, M., Economou, A., & Tagmatarchis, N. (2017).

Fabrication of a “green” and low-cost screen-printed graphene sensor and its application to the determination of caffeine by adsorptive stripping voltammetry. *International Journal of Electrochemical Science*, *12*(7), 6054–6067.

Li, C. H., Xiao, X., Tao, J., Wang, D. M., Huang, C. Z., & Zhen, S. J. (2017). A graphene oxide-based strand displacement amplification platform for ricin detection using aptamer as recognition element. *Biosensors and Bioelectronics*, *91*, 149–154.

Li, J., Ye, N., Gao, C., Zhou, T., & Ma, J. (2015). Capillary coated with graphene oxide as stationary phase for the separation of brucine and strychnine by capillary electrophoresis. *Journal of Chromatographic Science*, *53*(4), 641–645.

Lijinsky, W., & Kovatch, R. M. (1989). Chronic Toxicity Tests of Sodium Thiocyanate With Sodium Nitrite in F344 Rats. *Toxicology and Industrial Health*, *5*(1), 25–29.

Liu, C.-Y., & Tseng, W.-L. (2011). Colorimetric assay for cyanide and cyanogenic glycoside using polysorbate 40-stabilized gold nanoparticles. *Chemical Communications*, *47*(9), 2550–2552.

Liu, C.-Y., & Tseng, W.-L. (2012). Using polysorbate 40-stabilized gold nanoparticles in colorimetric assays of hydrogen cyanide in cyanogenic glycoside-containing plants. *Analytical Methods*, *4*(8), 2537.

Liu, Q., Shi, J., Zeng, L., Wang, T., Cai, Y., & Jiang, G. (2011). Evaluation of graphene as an advantageous adsorbent for solid-phase extraction with chlorophenols as model analytes. *Journal of Chromatography A*, *1218*(2), 197–204.

Liu, Y., Ai, K., Cheng, X., Huo, L., & Lu, L. (2010). Gold-nanocluster-based fluorescent sensors for highly sensitive and selective detection of cyanide in water. *Advanced Functional Materials*, *20*(6), 951–956.

Lou, X., Zeng, Q., Zhang, Y., Wan, Z., Qin, J., & Li, Z. (2012). Functionalized polyacetylenes with strong luminescence: “turn-on” fluorescent detection of cyanide based on the dissolution of gold nanoparticles and its application in real samples. *Journal of Materials Chemistry*, *22*(12), 5581–5586.

Lou, X., Zhang, Y., Qin, J., & Li, Z. (2011). A highly sensitive and selective fluorescent probe for cyanide based on the dissolution of gold nanoparticles and its application in real samples. *Chemistry - A European Journal*, *17*(35), 9691–9696.

Ly, S. Y., Lee, C. H., & Jung, Y. S. (2009). Voltammetric bioassay of caffeine using sensor implant. *NeuroMolecular Medicine*, *11*(1), 20–27.

Mahanthappa, M., Yellappa, S., Kottam, N., & Srinivasa Rao Vusa, C. (2016). Sensitive determination of caffeine by copper sulphide nanoparticles modified carbon paste electrode. *Sensors and Actuators, A: Physical*, *248*, 104–113.

Mahapatra, N., Datta, S., & Halder, M. (2014). A new spectroscopic protocol for selective detection of water soluble sulfides and cyanides: Use of Ag-nanoparticles synthesized by Ag(I)-reduction via photo-degradation of azo-food-colorants. *Journal of Photochemistry and Photobiology A: Chemistry*, *275*, 72–80.

Manfredi, A., Giannetto, M., Mattarozzi, M., Costantini, M., Mucchino, C., & Careri, M. (2016).

Competitive immunosensor based on gliadin immobilization on disposable carbon-nanogold screen-printed electrodes for rapid determination of celiotoxic prolamins. *Analytical and Bioanalytical Chemistry*, *408*(26), 7289–7298.

Mcl Mowat, A. (2003). Coeliac disease—a meeting point for genetics, immunology, and protein chemistry. *The Lancet*, *361*(9365), 1290–1292.

Migliaccio, E., Celentano, R., Viglietti, A., & Viglietti, G. (1990). Strychnine poisoning: A clinical case. *Minerva anestesiologica*, *56*(1–2), 41–42.

Momeni, S., Ahmadi, R., Safavi, A., & Nabipour, I. (2017). Blue-emitting copper nanoparticles as a fluorescent probe for detection of cyanide ions. *Talanta*, *175*, 514–521.

Nawrot, P., Jordan, S., Eastwood, J., Rotstein, J., Hugenholtz, A., & Feeley, M. (2003). Effects of caffeine on human health. *Food Additives & Contaminants*, *20*(1), 1–30.

Nilam, M., Hennig, A., Nau, W. M., & Assaf, K. I. (2017). Gold nanoparticle aggregation enables colorimetric sensing assays for enzymatic decarboxylation. *Anal. Methods*, *9*(19), 2784–2787.

Oke, O. L. (1979). Some aspects of the role of cyanogenic glycosides in nutrition. In *Some Special Aspects of Nutrition* (Vol. 33, pp. 70–103). Karger Publishers.

Peeters, M., Van Grinsven, B., Cleij, T. J., Jiménez-Monroy, K. L., Cornelis, P., Pérez-Ruiz, E., … Wagner, P. (2015). Label-free protein detection based on the heat-transfer method-a case study with the peanut allergen Ara h 1 and aptamer-based synthetic receptors. *ACS Applied Materials and Interfaces*, *7*(19), 10316–10323.

Peng, Y., Zhang, W., Chang, J., Huang, Y., Chen, L., Deng, H., … Wen, Y. (2017). A simple and sensitive method for the voltammetric analysis of theobromine in food samples using nanobiocomposite sensor. *Food Analytical Methods*, *10*(10), 3375–3384.

Peters, J. M. (1967). Factors affecting caffeine toxicity: a review of the literature. *The Journal of Clinical Pharmacology*, *7*(3), 131–141.

Pfizer Pharmaceuticals Group. (2006). *Material safety data sheet: Codeine poly(styrene-divinylbenzene) sulfonate syrup*. Retrieved from http://www.haskellcorp.com/uploads/msds/Gases/chevron regular unleaded gasoline.pdf Accessed 02 September 2018.

Pfizer Pharmaceuticals Group. (2007). *Material Safety Data Sheet: Ephedrine/theophylline/hydroxyzine hydrochloride tablets*. Retrieved from http://www.pfizer.com/files/products/material_safety_data/257.pdf Accessed 02 September 2018.

Pfizer Pharmaceuticals Group. (2013). *Material safety data sheet: Diphenoxylate hydrochloride and atropine sulfate liquid*. Retrieved from http://www.pfizer.com/system/files/products/material_safety_data/DIPHENOXYLATE AND ATROPINE.pdf Accessed 02 September 2018.

Qing, Z., Hou, L., Yang, L., Zhu, L., Yang, S., Zheng, J., & Yang, R. (2016). A reversible nanolamp for instantaneous monitoring of cyanide based on an Elsner-like reaction. *Analytical Chemistry*, *88*(19), 9759–9765.

Rezaei, B., Khalili Boroujeni, M., & Ensafi, A. A. (2014). Caffeine electrochemical sensor using imprinted film as recognition element based on polypyrrole, sol-gel, and gold nanoparticles hybrid nanocomposite modified pencil graphite electrode. *Biosensors and Bioelectronics*, *60*, 77–83.

Savalia, R., & Chatterjee, S. (2017). Sensitive detection of brucine an anti-metastatic drug for hepatocellular carcinoma at carbon nanotubes – nafion composite based biosensor. *Biosensors and Bioelectronics*, *98*, 371–377.

Sereshti, H., Khosraviani, M., Samadi, S., & Amini-Fazl, M. S. (2014). Simultaneous determination of theophylline, theobromine and caffeine in different tea beverages by graphene-oxide based ultrasonic-assisted dispersive micro solid-phase extraction combined with HPLC-UV. *RSC Adv.*, *4*(87), 47114–47120.

Shibamoto, T., & Bjeldanes, L. F. (2009). *Introduction to food toxicology*. Cambridge: Academic press.

Shu, X., Bian, F., Wang, Q., Qin, X., & Wang, Y. (2017). Electrochemical sensor for simultaneous determination of theophylline and caffeine based on a novel poly(folic acid)/graphene composite film modified electrode. *International Journal of Electrochemical Science*, *12*(5), 4251–4264.

Song, J., Wu, F.-Y., Wan, Y.-Q., & Ma, L.-H. (2015). Ultrasensitive turn-on fluorescent detection of trace thiocyanate based on fluorescence resonance energy transfer. *Talanta*, *132*, 619–624.

Staiano, M., Matveeva, E. G., Rossi, M., Crescenzo, R., Gryczynski, Z., Gryczynski, I., … Dauria, S. (2009). Nanostructured silver-based surfaces: New emergent methodologies for an easy detection of analytes. *ACS Applied Materials and Interfaces*, *1*(12), 2909–2916.

Sun, J. Y., Huang, K. J., Wei, S. Y., & Wu, Z. W. (2011). Application of cetyltrimethylammonium bromide – graphene modified electrode for sensitive determination of caffeine. *Canadian Journal of Chemistry*, *89*(6), 697–702.

Sun, J. Y., Huang, K. J., Wei, S. Y., Wu, Z. W., & Ren, F. P. (2011). A graphene-based electrochemical sensor for sensitive determination of caffeine. *Colloids and Surfaces B: Biointerfaces*, *84*(2), 421–426.

Sun, X., Jia, M., Guan, L., Ji, J., Zhang, Y., Tang, L., & Li, Z. (2015). Multilayer graphene-gold nanocomposite modified stem-loop DNA biosensor for peanut allergen-Ara h1 detection. *Food Chemistry*, *172*, 335–342.

Sun, X., Jia, M., Ji, J., Guan, L., Zhang, Y., Tang, L., & Li, Z. (2015). Enzymatic amplification detection of peanut allergen Ara h1 using a stem-loop DNA biosensor modified with a chitosan-mutiwalled carbon nanotube nanocomposite and spongy gold film. *Talanta*, *131*, 521–527.

Sundramoorthy, A. K., Sadak, O., Anandhakumar, S., & Gunasekaran, S. (2016). Synthesis of poly(8-aminopyrene-1,3,6-trisulfonic acid)/CNT nanocomposite for electrochemical detection of caffeine. *Journal of The Electrochemical Society*, *163*(13), B638–B643.

Szlag, V. M., Styles, M. J., Madison, L. R., Campos, A. R., Wagh, B., Sprouse, D., … Haynes, C. L.

(2016). SERS Detection of ricin B-Chain via N-Acetyl-Galactosamine Glycopolymers. *ACS Sensors*, *1*(7), 842–846.

Talio, M. C., Acosta, M. G., Alesso, M., Luconi, M. O., & Fernández, L. P. (2014). Quantification of caffeine in dietary supplements and energy drinks by solid-surface fluorescence using a pre-concentration step on multi-walled carbon nanotubes and Rhodamine B. *Food Additives and Contaminants - Part A Chemistry, Analysis, Control, Exposure and Risk Assessment*, *31*(8), 1367–1374.

Tang, J. J., Sun, J. F., Lui, R., Zhang, Z. M., Liu, J. F., & Xie, J. W. (2016). New surface-enhanced Raman sensing chip designed for on-site detection of active ricin in complex matrices based on specific depurination. *ACS Applied Materials and Interfaces*, *8*(3), 2449–2455.

Thabano, J. R. E., Breadmore, M. C., Hutchinson, J. P., Johns, C., & Haddad, P. R. (2009). Silica nanoparticle-templated methacrylic acid monoliths for in-line solid-phase extraction-capillary electrophoresis of basic analytes. *Journal of Chromatography A*, *1216*(25), 4933–4940.

Tran, D. T., Knez, K., Janssen, K. P., Pollet, J., Spasic, D., & Lammertyn, J. (2013). Selection of aptamers against Ara h 1 protein for FO-SPR biosensing of peanut allergens in food matrices. *Biosensors and Bioelectronics*, *43*(1), 245–251.

Trani, A., Petrucci, R., Marrosu, G., Zane, D., & Curulli, A. (2017). Selective electrochemical determination of caffeine at a gold-chitosan nanocomposite sensor: May little change on nanocomposites synthesis affect selectivity? *Journal of Electroanalytical Chemistry*, *788*, 99–106.

Tuerk, C., & Gold, L. (1990). Systematic evolution of ligands by exponential enrichment: RNA ligands to bacteriophage T4 DNA polymerase. *Science (New York, N.Y.)*, *249*(4968), 505–510.

U.S. Department of Energy. (2008). *Temporary emergency exposure limits for chemicals: Methods and practice*. *U.S. Department of Energy*.

U.S. Department of Health and Human Services. (2007). *NIOSH pocket guide to chemical hazards*. *DHHS (NIOSH)*.

Vasilescu, I., Eremia, S. A. V, Penu, R., Albu, C., Radoi, A., Litescu, S. C., & Radu, G.-L. (2015). Disposable dual sensor array for simultaneous determination of chlorogenic acid and caffeine from coffee. *RSC Adv.*, *5*(1), 261–268.

Velmurugan, M., Karikalan, N., Chen, S. M., & Karuppiah, C. (2016). Core-shell like Cu2O nanocubes enfolded with Co(OH)2 on reduced graphene oxide for the amperometric detection of caffeine. *Microchimica Acta*, *183*(10), 2713–2721.

Wang, C. W., Chen, Y. N., Wu, B. Y., Lee, C. K., Chen, Y. C., Huang, Y. H., & Chang, H. T. (2016). Sensitive detection of cyanide using bovine serum albumin-stabilized cerium/gold nanoclusters. *Analytical and Bioanalytical Chemistry*, *408*(1), 287–294.

Wang, L., Zheng, J., Yang, S., Wu, C., Liu, C., Xiao, Y., … Yang, R. (2015). Two-photon sensing and imaging of endogenous biological cyanide in plant tissues using graphene quantum dot/gold nanoparticle conjugate. *ACS Applied Materials and Interfaces*, *7*(34), 19509–19515.

Wang, S., Lei, Y., Zhang, Y., Tang, J., Shen, G., & Yu, R. (2010). Hydroxyapatite nanoarray-based

cyanide biosensor. *Analytical Biochemistry*, *398*(2), 191–197.

Wang, T. Y., Chen, C. Y., Wang, C. M., Tan, Y. Z., & Liao, W. S. (2017). Multicolor functional carbon dots via one-step refluxing synthesis. *ACS Sensors*, *2*(3), 354–363.

Wang, Y., Ding, Y., Li, L., & Hu, P. (2018). Nitrogen-doped carbon nanotubes decorated poly (L-Cysteine) as a novel, ultrasensitive electrochemical sensor for simultaneous determination of theophylline and caffeine. *Talanta*, *178*, 449–457.

Wang, Y., Wei, X., Wang, F., & Li, M. (2014). Sensitive voltammetric detection of caffeine in tea and other beverages based on a DNA-functionalized single-walled carbon nanotube modified glassy carbon electrode. *Analytical Methods*, *6*, 7525–7531. http://doi.org/10.1039/c4ay00837e

Wei, S., Hsu, P., Lee, Y., Lin, Y., & Huang, C. (2012). Selective detection of iodide and cyanide anions using gold-nanoparticle-based fluorescent probes. *ACS Applied Materials & Interfaces*, *4*, 2652–2658.

Weng, X., & Neethirajan, S. (2016). A microfluidic biosensor using graphene oxide and aptamer-functionalized quantum dots for peanut allergen detection. *Biosensors and Bioelectronics*, *85*, 649–656.

White, S. P., Sreevatsan, S., Frisbie, C. D., & Dorfman, K. D. (2016). Rapid, Selective, Label-Free Aptameric Capture and Detection of Ricin in Potable Liquids Using a Printed Floating Gate Transistor. *ACS Sensors*, *1*(10), 1213–1216.

World Health Organization. (1991). Coffee, tea, mate methylxanthines and methylglyoxal. In *IARC monographs on the evaluation of the carcinogenic risk of chemicals to humans* (Vol. 51, p. 432). Lyon: IARC.

World Health Organization. (1996). Cyanide in drinking-water. In *Guidelines for drinking-water quality* (2nd ed., Vol. 2, pp. 1–4). Geneva: World Health Organization.

Xiao, X., Li, Y. F., Huang, C. Z., & Zhen, S. J. (2015). A novel graphene oxide amplified fluorescence anisotropy assay with improved accuracy and sensitivity. *Chemical Communications (Cambridge, England)*, *51*(89), 16080–16083.

Xiao, X., Tao, J., Zhang, H. Z., Huang, C. Z., & Zhen, S. J. (2016). Exonuclease III-assisted graphene oxide amplified fluorescence anisotropy strategy for ricin detection. *Biosensors and Bioelectronics*, *85*, 822–827.

Yang, L., Ran, X., Cai, L., Li, Y., Zhao, H., & Li, C. P. (2016). Calix[8]arene functionalized single-walled carbon nanohorns for dual-signalling electrochemical sensing of aconitine based on competitive host-guest recognition. *Biosensors and Bioelectronics*, *83*, 347–352.

Yang, S., Yang, R., Li, G., Qu, L., Li, J., & Yu, L. (2010). Nafion/multi-wall carbon nanotubes composite film coated glassy carbon electrode for sensitive determination of caffeine. *Journal of Electroanalytical Chemistry*, *639*(1–2), 77–82.

Ye, N., Li, J., Gao, C., & Xie, Y. (2013). Simultaneous determination of atropine, scopolamine, and anisodamine in Flos daturae by capillary electrophoresis using a capillary coated by graphene oxide. *Journal of Separation Science*, *36*(16), 2698–2702.

Yin, H. Q., Jia, M. X., Yang, S., Wang, S. Q., & Zhang, J. G. (2012). A nanoparticle-based

bio-barcode assay for ultrasensitive detection of ricin toxin. *Toxicon*, *59*(1), 12–16.

Yin, H. Y., Chu, P. T., Tsai, W. C., & Wen, H. W. (2016). Development of a barcode-style lateral flow immunoassay for the rapid semi-quantification of gliadin in foods. *Food Chemistry*, *192*, 934–942.

Zengin, A., Tamer, U., & Caykara, T. (2015). Fabrication of a SERS based aptasensor for detection of ricin B toxin. *Journal of Materials Chemistry B*, *3*, 306–315.

Zhai, Y., Jin, L., Wang, P., & Dong, S. (2011). Dual-functional Au–Fe_3O_4 dumbbell nanoparticles for sensitive and selective turn-on fluorescent detection of cyanide based on the inner filter effect. *Chemical Communications*, *47*(29), 8268–8270.

Zhang, C., Han, Y., Lin, L., Deng, N., Chen, B., & Liu, Y. (2017). Development of quantum dots-labeled antibody fluorescence immunoassays for the detection of morphine. *Journal of Agricultural and Food Chemistry*, *65*(6), 1290–1295.

Zhang, H. F., & Shi, Y. P. (2012). Preparation of Fe3O4 nanoparticle enclosure hydroxylated multi-walled carbon nanotubes for the determination of aconitines in human serum samples. *Analytica Chimica Acta*, *724*, 54–60.

Zhang, J., Wang, L. P., Guo, W., Peng, X. D., Li, M., & Yuan, Z. B. (2011). Sensitive Differential Pulse Stripping Voltammetry of Caffeine in M edicines and Cola Using a Sensor Based on M ulti-Walled Carbon Nanotubes and Nafion. *International Journal of Electrochemical Science*, *6*, 997–1006.

Zhang, Y., Liu, Y., Zhen, S. J., & Huang, C. Z. (2011). Graphene oxide as an efficient signal-to-background enhancer for DNA detection with a long range resonance energy transfer strategy. *Chemical Communications (Cambridge, England)*, *47*(42), 11718–20.

Zhao, F., Wang, F., Zhao, W., Zhou, J., Liu, Y., Zou, L., & Ye, B. (2011). Voltammetric sensor for caffeine based on a glassy carbon electrode modified with Nafion and graphene oxide. *Microchimica Acta*, *174*(3), 383–390.

Zhu, D., Li, W., Wen, H. M., Hu, Y., Wang, J., Zhu, J. M., … Gu, C. Q. (2015). Development of polyacrylic acid-functionalized porous zinc sulfide nanospheres for a non-aqueous solid phase extraction procedure toward alkaloids. *RSC Advances*, *5*(38), 29820–29827.

Zhu, D., Miao, Z. Y., Yang, R. X., Wen, H. M., Li, W., Chen, J., … Hu, Y. (2016). Layer-by-layer functionalized porous Zinc sulfide nanospheres-based solid-phase extraction combined with liquid chromatography time-of- flight/mass and gas chromatography-mass spectrometry for the specific enrichment and identification of alkaloids from *Crinum asiaticum* var. *sinicum*. *Analytica Chimica Acta*, *932*, 60–68.

Legends of Figures

Fig. 1 Schematic representation of four detection assays of protein. Two possible set-ups of electrochemical immunosensors producing signals in positive (A) or negative (B) correlation with the target amount. Two fluorescence detection of ricin B-chain, including a Graphene oxide-based strand displacement amplification platform (C) (C. H. Li et al., 2017; copyright 2017 Elsevier) and an exonuclease III-assisted graphene oxide amplified fluorescence anisotropy strategy (D) (Xiao et al., 2016; copyright 2016 Elsevier).

Fig. 2 Multifunctional nanomaterials in four phases of determining phytotoxins from various plants and food products. Fe*, Fe_2O_4 and Fe_3O_4 nanoparticles (NPs) and magnetic beads; CNT, single-walled and multi-walled carbon nanotubes; CNC, carbon nanocages; Si*, silica NPs and nanospheres; GO*, graphene oxide (GO), reduced GO (rGO), and porous rGO (prGO); Gr, graphene; Au*, gold NPs, nanoclusters, and film-over-nanospheres; Cu*, copper NPs, CuS NPs, and Cu_2O nanocubes; QD, quantum dots; CD: carbon dots; HA, hydroxyapatite; Ag*, silver NPs, silver island films, and silver dendrite nanosubstrate; Al*, nanoporous aluminum substrate; Si*: silica NPs and nanospheres; Apt; aptamer; IMLN: immunoliposomal nanovesicles.

Table(s)

Table 1. Oral median lethal doses and human exposure limits of some representative phytotoxins.

Phytotoxins	Oral LD_{50}	Ref.	Human exposure limit	Regulatory organization	Ref.
Alkaloids					
Caffeine	150–200 mg/kg (human)	(Peters, 1967)	6 mg/kg	Bureau of Chemical Safety, Canada	(Nawrot et al., 2003)
Theophylline	225 mg/kg (rat)	(Pfizer Pharmaceuticals Group, 2007)	TWA[a] 1.8mg/m³	Pfizer Ltd., U.K.	(Pfizer Pharmaceuticals Group, 2007)
Theobromine	950 mg/kg (rat)	(World Health Organization, 1991)	39.05 mg/day	World Health Organization (WHO)	(World Health Organization, 1991)
Brucine	1 mg/kg (rat)	(Gleason, Gosselin, & Hodge, 1957)	/[b]	/	/
Strychnine	30–100 mg/kg (human)	(Migliaccio, Celentano, Viglietti, & Viglietti, 1990)	TWA 0.15 mg/m^3	National Institute for Occupational Safety and Health, U.S.A.; Occupational Safety and Health Administration, U.S.A.	(U.S. Department of Health and Human Services, 2007)
Morphine	335 mg/kg (rat)	(Lewis & Sax, 2004)	10 µg /kg	European Food Safety Authority	(Knutsen et al., 2018)
Codeine	427 mg/kg (rat)	(Pfizer Pharmaceuticals Group, 2006)	TWA 0.07 mg/m³	Pfizer Ltd., U.K.	(Pfizer Pharmaceuticals Group, 2006)
Atropine	500 mg/kg (rat)	(Lewis & Sax, 2004)	TWA 2.5 µg/m³	Pfizer Ltd., U.K.	(Pfizer Pharmaceuticals Group, 2013)
Colchicine	<0.8 mg/kg (human)	(Hirayama, Hiruma, Ueda, Doi, & Morimura, 2018)	/	/	/
Cyanides					
Hydrogen cyanide	1.52 mg/kg (human)	(Agency for Toxic Substances and Disease Registry, 1989)	Cyanide ions: 0.07 mg/L in drinking water	WHO	(World Health Organization, 1996)
Sodium thiocyanate	750 mg/kg (rat)	(Lijinsky & Kovatch, 1989)			
Linamarin	450 mg/kg (rat)	(Oke, 1979)			
Cyanamide	125 mg/kg (rat)	(Lewis & Sax, 2004)	TWA 2 mg/m³	National Institute for Occupational Safety and Health, U.S.A	(U.S. Department of Health and Human Services, 2007)
Proteins					
Ricin	<1 mg/kg (human)	(European Food Safety Authority, 2008)	0.025 mg/m^3	U.S. Department of Energy	(U.S. Department of Energy, 2008)
Abrin	0.01–1 mg/kg (human)	(Johnson et al., 2009)	/	/	/

[a] TWA: Time-weighted average.

[b] Data not available.

Table 2. Representative nanomaterial-based assay for the detection of plant-derived toxic alkaloids in foods[a].

Analyte	Nanomaterial (in conjugation)	Role of nanomaterial	Detection technique	Signal/ Target[b]	LOD[c] (μM)	LOQ[d] (μM)	Linear range[e] (μM)	Sample	Reference
Caffeine	MWCNTs	GCE coating	SWV	+	3.52×10^{-3}	/[f]	10–500	Tea leaves, coffee, cold drink	(Gupta, Jain, & Shoora, 2013)
Caffeine	PLCY/N-MWCNTs	GCE coating	DPV	+	0.2	/	0.4–140	Green tee, energy drink	(Yingzi Wang, Ding, Li, & Hu, 2018)
Caffeine	Naf/MWCNTs	GCE coating	DPV	+	2.3×10^{-4}	/	6.0×10^{-4}–0.4	Cola, energy drink, green tea	(Yang et al., 2010)
Caffeine	Naf/MWCNTs	GCE coating	DPV	+	0.513	/	2.945–377; 377–2356	Cola	(J. Zhang et al., 2011)
Caffeine	CHIT-MWCNTs	GCE coating	DPV	+	0.04	/	< 7000	Commercial beverages	(Carolina Torres, Barsan, & Brett, 2014)
Caffeine	HTAB-MWCNTs	Sorbent	Fluorescence	+	0.3 μg/L	1.1 μg/L	$1.1–9.7\times10^{3}$ μg/L	Energy drinks, tea	(Talio, Acosta, Alesso, Luconi, & Fernández, 2014)
Caffeine	Fe_3O_4-MWCNTs	Sorbent	SWV	+	0.05	/	0.5–20	Energy drink, soft drink, chocolate milk	(Filik & Aslıhan Avan, 2018)
Caffeine	SWCNTs	CCE coating	DPV	+	0.25	/	0.4–300	Coca cola, Pepsi cola, tea	(Habibi, Abazari, & Pournaghi-Azar, 2014)
Caffeine	DNA-SWCNTs	Electrode	SWASV	+	0.35	/	1.0×10^{2}–1.2×10^{4} μg/L	Black tea tree leaf	(Ly, Lee, & Jung, 2009)
Caffeine	Naf/DNA-SWCNTs	GCE coating	SWASV	+	1.0×10^{-4}	/	5.0×10^{-4}–0.1	Green tea, black tea, oolong tea, cola, energy drink	(Yanwei Wang, Wei, Wang, & Li, 2014)
Caffeine	poly(APTA)/SWCNTs	GCE coating	Amperometry	+	10	/	10–760	Raspberry fruit tea	(Sundramoorthy, Sadak, Anandhakumar, & Gunasekaran, 2016)
Caffeine	N-Gr–N-CNTs	GCE coating	SWV	+	0.02	/	0.06–50	Cookie, chocolate, milk tea	(Jiang, Ding, Jiang, Li, & Mo, 2014)
Caffeine	GO	Sorbent	UAD-μ-SPE-HPLC-UV	+	0.11–0.90 μg/L	0.37–3.00 μg/L	3.0–5000	Black, white, oolong, and green teas	(Sereshti, Khosraviani, Samadi, & Amini-Fazl, 2014)
Caffeine	Naf/GO	GCE coating	DPV	+	2.0×10^{-4}	/	4.0×10^{-4}–8.0×10^{-2}	Cola, tea, energy drink	(Zhao et al., 2011)
Caffeine	rGO	Electrode	DPV	+	/	/	50–300	Soluble coffee, cola, tea, decaffeinated tea	(Khoo, Pumera, & Bonanni, 2013)
Caffeine	Naf/rGO	CSPE coating	Amperometry	+	0.22	/	0.29–2.58	Commercial coffee samples	(Vasilescu et al., 2015)
Caffeine	rGO/Cu_2O/$Co(OH)_2$ nanocubes	GCE coating	Amperometry	+	0.4	/	0.83–1200	Soluble coffee powder, cola beverage, energy drinks	(Velmurugan, Karikalan, Chen, & Karuppiah, 2016)
Caffeine	CTAB–Gr	GCE coating	DPV	+	9.1×10^{-2}	/	0.3–100	Coca-Cola; Pepsi Cola;	(Sun, Huang, Wei, & Wu, 2011)

								energy drink; instant coffee; commercial coffee samples	
Caffeine	Naf/Gr	GCE coating	DPV	+	0.12	/	4.0×10^{-4}–4.0×10^{-2}; 4.0×10^{-2}–6.0×10^{-1}	Cola, energy drink, instant coffee, commercial coffee	(Sun, Huang, Wei, Wu, & Ren, 2011)
Caffeine	Naf/Gr	CSPE coating	SWASV	+	0.021	0.066	0.10–0.90; 1.0–10	Cola, energy drink, coffee, ice tea	(Lezi, Economopoulos, Prodromidis, Economou, & Tagmatarchis, 2017)
Caffeine	PFA/Gr	GCE coating	DPV	+	0.03	/	0.2–10; 10–100	Black tea, green tea, Coca Cola, energy drink	(Shu, Bian, Wang, Qin, & Wang, 2017)
Caffeine	CNC	Sorbent	UV-vis spectroscopy	+	/	/	/	Tea	(Ariga, Vinu, Miyahara, Hill, & Mori, 2007)
Caffeine	BCDs	Fluorophore	Fluorescence	-	/	/	1–75	Sprite	(T. Y. Wang, Chen, Wang, Tan, & Liao, 2017)
Caffeine	Au NPs	MIP/PGE coating	SWV	+	0.9×10^{-3}	/	0.2×10^{-2}–0.5×10^{-1}; 0.5×10^{-1}–1	Soft drink, energy drink, green tea	(Rezaei, Khalili Boroujeni, & Ensafi, 2014)
Caffeine	Au NP-CHIT	Au electrode coating	DPV	+	1.0	/	2.0–5000	Energy drink, soft drink, tea	(Trani, Petrucci, Marrosu, Zane, & Curulli, 2017)
Caffeine	CuS NPs	CPE coating	DPV	+	1.86×10^{-2}	6.22×10^{-2}	2–120	Green tea, black tea, Bru coffee, Nescafe	(Mahanthappa, Yellappa, Kottam, & Srinivasa Rao Vusa, 2016)
Caffeine	Si NPs	Monolith etching	In-line SPE-CE	+	/	/	/	“Caffeine-free” cola	(Thabano, Breadmore, Hutchinson, Johns, & Haddad, 2009)
Theophylline	PLCY/N-MWCNTs	GCE coating	DPV	+	0.033	/	0.1–70	Green tea, energy drink	(Yingzi Wang et al., 2018)
Theophylline	PFA/Gr	GCE coating	DPV	+	0.08	/	1–10; 10–160	Black tea	(Shu et al., 2017)
Theobromine	GO	Sorbent	UAD-μ-SPE-HPLC-UV	+	0.90 ng/L	3.00 ng/L	0.003–5μg/L	Black, white, oolong, and green teas	(Sereshti et al., 2014)
Theobromine	GO	Sorbent	UAD-μ-SPE-HPLC-UV	+	0.11 ng/L	0.37 ng/L	0.001–5μg/L	Black, white, oolong, and green teas	(Sereshti et al., 2014)
Theobromine	CMC-MWCNTs	GCE coating	LSV	+	0.21	/	0.5–80	Green tea, chocolate, coffee	(Peng et al., 2017)
Theobromine	CMC-MWCNTs	GCE coating	LSV	+					(Peng et al., 2017)
Codeine	SWCNTs	CCE coating	DPV	+	0.11	/	0.2–230	Coca cola, Pepsi cola, tea	(Habibi et al., 2014)

Atropine	MWCNTs	Electrode	DPV	+	0.449 µg/L	4.498 µg/L	3.98–27.23 µg/L	*Datura stramonium* seed and leaves	(Dar, Brahman, Tiwari, & Pitre, 2012)
Atropine	GO	Capillary coating	CE-PAD	+	5.0×10^{2} µg/L	/	5.0×10^{2}–2.0×10^{5} µg/L	*Flos daturae*	(Ye, Li, Gao, & Xie, 2013)
Strychnine	MWCNTs	CPE coating	DPV	+	0.43	/	50–1000	*Strychnos nux-vomica* crude and detoxified seeds, cow's milk	(Behpour, Ghoreishi, Khayatkashani, & Motaghedifard, 2012)
Strychnine	Au NPs	CPE coating	DPV	+	0.46	/	8–35; 35–1150	*Strychnos nux-vomica* crude and processed seeds	(Behpour, Ghoreishi, Khayatkashani, & Motaghedifar, 2011)
Brucine	MWCNTs	CPE coating	DPV	+	0.28	/	5–355	*Strychnos nux-vomica* crude and detoxified seeds, cow's milk	(Behpour et al., 2012)
Brucine	Naf/SWCNTs	GCE coating	SWV	+	1.1×10^{-4}	/	1.0×10^{-3}–8.0	*S. nux-vomica* seeds	(Savalia & Chatterjee, 2017)
Morphine	CdTe/ZnS QDs	Fluorophore; bind to Ab	Plate-FLISA	-	0.27 µg/L	/	0.32–1000 µg/L	Hotpot soup base	(C. Zhang et al., 2017)
Colchicine	MOF-5(Zn)-Fe_2O_4 NPs	Magnetic concentration	UAD-MSPME-HPLC-UV	+	0.13 µg/L	0.43 µg/L	0.5–1700 µg/L	Colchicine autumn and spring roots	(Bahrani et al., 2017)

[a]Abbreviations: LOD, limit of detection; LOQ, limit of quantification; MWCNTs, multi-walled carbon nanotubes; GCE, glassy carbon electrode; SWV, square wave voltammetry; PLCY, poly (L-cysteine); N, nitrogen-doped; DPV, differential pulse voltammetry; Naf, Nafion; CHIT, chitosan; HTAB, hexadecyl-trimethylammonium bromide; SWCNTs, single-walled carbon nanotubes; SWASV, square wave adsorptive stripping voltammetry; APTA, 8-aminopyrene-1,3,6-trisulfonic acid; Gr, graphene; GO, graphene oxide; UAD-µ-SPE-HPLC-UV, ultrasound-assisted dispersive micro-solid phase extraction followed by high performance liquid chromatography-ultraviolet detection; rGO, reduced graphene oxide; CSPE, carbon screen-printed electrode; CTAB, cetyltrimethylammonium bromide; PFA, poly (folic acid); CNC, carbon nanocage; BCDs, blue carbon dots; Au NPs, gold nanoparticles; MIP/PGE, molecularly imprinted polymer-coated pencil graphite electrode; SPE-CE, solid phase extraction coupled with capillary electrophoresis; LSV: linear sweep voltammetry; PAD, photodiode array detector; QDs, quantum dots; Abs, antibodies; FLISA, fluorescence immunosorbent assay; MOF, metal organic framework; MSPME, magnetic solid phase microextraction.

[b]Positive (+) or negative (-) correlation between signal and target.

[c–e]Shown in µM unless specified.

[f] Data not available.

Table 3. Representative nanomaterial-based assay for the detection of plant-derived cyanides in foods[a].

Analyte	Nanomaterial	Role of nanomaterial	Detection technique	Signal/ Target[b]	LOD[c] (μM)	LOQ[d] (μM)	Linear range[e] (μM)	Sample	Reference
Cyanide	PS 40–Au NPs	Reducing agent	Colorimetry	+	/	/	0–2.5	Cassava roots, peach kernels, and loquat kernels	(C.-Y. Liu & Tseng, 2012)
Cyanide	FITC–BSA–Au NPs	Reducing and quenching agent	Fluorescence	+	1.0	/	0–10	Pond water, tap water, and seawater	(Wei, Hsu, Lee, Lin, & Huang, 2012)
Cyanide	Polyfluorene–Au NPs	Reducing and quenching agent	Fluorescence	+	/	3.0×10^{-4}	$0–1.3\times10^{-1}$	Groundwater, tap water, boiled water, and lake water	(Lou, Zhang, Qin, & Li, 2011)
Cyanide	PA–Au NPs	Reducing and quenching agent	Fluorescence	+	/	/	$0–9.3\times10^{-1}$	Groundwater, tap water, boiled water, and lake water,	(Lou et al., 2012)
Cyanide	ATP–AuNPs	Color source	Colorimetry	+	59 μg/L	170 μg/L	-	Mineral water	(González-Castro, Peña-Vázquez, & Bermejo-Barrera, 2015)
Cyanide	BSA–Ce/Au NCs	Reducing agent; fluorophore	Fluorescence	+	5.0×10^{4}	/	0.1–15	Pond water and drinking water	(C. W. Wang et al., 2016)
Cyanide	BSA–Au NCs	Reducing agent; fluorophore	Fluorescence	-	/	200×10^{-6}	200×10^{-6}–9.5×10^{-3}	Local groundwater, tap water, pond water, and lake water	(Y. Liu, Ai, Cheng, Huo, & Lu, 2010)
Cyanide	Au NP–peptide@GrQDs	AuNPs: reducing and quenching agent; GrQDs: fluorophore	Fluorescence	+	0.52	/	1–200	Cassava root, potato, sweet potato, and purple sweet potato	(L. Wang et al., 2015)
Cyanide	Au–Fe_3O_4 NPs	Au NPs: reducing and quenching agent; Fe_3O_4 NPs: magnetic	Fluorescence	+	4.0×10^{-4}	/	0.4×10^{-3}–1.2×10^{-1}	Tap water, ground water, and lake water	(Zhai, Jin, Wang, & Dong, 2011)

		concentration							
Cyanide	C314-Ag NPs	C314: fluorophore; Ag NPs: reducing and quenching agent	Fluorescence	+	60 μg/L	/	0–100	Pond water, tap water	(Mahapatra, Datta, & Halder, 2014)
Cyanide	Cu NPs	Reducing agent; fluorophore	Fluorescence	-	0.37	/	0.5–18	River water	(Momeni, Ahmadi, Safavi, & Nabipour, 2017)
Cyanide	dsDNA–Cu NPs	Reducing agent	Fluorescence	+	1.96	/	2.5–20	Cassava, sweet potato, and potato	(Qing et al., 2016)
Cyanide	CHIT–HRP/HANWA	GCE coating	Chronoamperometry	-	0.6 μg/L	/	8–20 μg/L	Tap water, river water, distilled wine, and cassava starch	(S. Wang et al., 2010)
Cyanamide	MWCNTs	Sorbent	LC-MS/MS	+	/	0.01, 0.05 mg/kg	/	21 kinds of plant-derived foods	(Cheng et al., 2018)
Thiocyanate	FTTC–Au NPs	Reducing and quenching agent	Fluorescence	+	90	/	1.0×10^{3}–4.0×10^{4}	Milk	(Song, Wu, Wan, & Ma, 2015)
Linamarin	PS 40-Au NPs	Reducing agent; color source	Colorimetry	+	/	/	1–2500 nM	Cassava root	(C.-Y. Liu & Tseng, 2011)

[a]Abbreviations: LOD, limit of detection; LOQ, limit of quantification; PS 40, Polysorbate 40; Au NPs, gold nanoparticles; FITC, fluorescein isothiocyanate; BSA, bovine serum albumin; PA, polyacetylene; ATP, adenosine triphosphate; Au NCs, gold nanoclusters; GrQDs, graphene quantum dots; C314, coumarin 314; Ag NPs, silver nanoparticles; Cu NPs, copper nanoparticles; dsDNA, double-stranded deoxyribonucleic acid; CHIT, chitosan; HRP, horseradish peroxidase; HANWA, hydroxyapatite nanowires array; GCE, glassy carbon electrode; MWCNTs, multi-walled carbon nanotubes.

[b]Positive (+) or negative (-) correlation between signal and target.

[c–e]Shown in μM unless specified.

Table 4. Representative nanomaterial-based assay for the detection of plant-derived toxic or allergenic proteins and corresponding DNAs in foods[a].

Analyte	Nanomaterial (in conjugation)	Role of nanomaterial	Detection technique	Signal/ Target[b]	LOD[c] (ng/mL)	LOQ[d] (ng/mL)	Linear range[e] (ng/mL)	Sample	Reference
Proteins									
Ricin	Apt	Recognizes target	DPV	+	1	/	/	Orange juice, milk	
Ricin	$KGdF_4:Eu^{3+}$ NPs−Apt; GO	$KGdF_4:Eu^{3+}$ NPs: fluorophore Apt: recognizes target; GO: quenching agent	Fluorescence	+	0.08	/	0.05–50	Portable water	(Huang et al., 2015)
Ricin	poly(21dA)−Au NPs@SH−Si; Ag nanoshell	Au NPs: platform of poly(21dA) that reacts with ricin; Ag nanoshell: signal amplifier	SERS	-	0.8	/	10–500	Drinking water, apple juice	(Tang et al., 2016)
Ricin	Ag dendrite nanosubstrate	Signal amplifier	SERS	+	4000	4000	/	Milk	(He, Deen, et al., 2011)
Ricin	Nanoporous Al substrate	Platform of anti-ricin Ab	EIS	+	/	/	/	Milk, vegetable soup, tomato juice	(Chai, Lee, & Takhistov, 2010)
RBC	ssDNA−Apt−MB; GO	Apt: recognizes target; MB: magnetic separation; GO: quenching agent	Fluorescence	+	6.0×10^2	/	7.5×10^2–1.0×10^5	Orange juice, caster beans	(Li et al., 2017)
RBC	ssDNA−Apt−MB; ssDNA−GO	Apt: recognizes target; MB: magnetic separation; GO: FA amplifier	FA measurement	-	400	/	1.0–13.3	Orange juice	(Xiao, Tao, Zhang, Huang, & Zhen, 2016)
RBC	Si–poly(AVAL)–Apt; Apt–Ag NPs−Bpy	Apt: recognizes target; Ag NPs: bind to aptamer and Bpy (Raman reporter) as SERS probe	SERS	+	0.32 pM	/	1.0 pM–50 fM	Orange juice, milk	(Zengin, Tamer, & Caykara, 2015)
RBC	Ag NPs−Apt	Ag NPs: bind to aptamer; Apt: recognizes target	SERS	+	10	/	/	Orange juice, milk	(He, Lamont, et al., 2011)

RBC	Au FONs-Si nanospheres	Platform for pNAGEMA to bind to RBC	SERS	+	20	80	/	Apple juice, orange juice	(Szlag et al., 2016)
RAC	AuNPs; MMP	Au NPs: link Ab and barcode DNA; MMP: magnetic separation	Real-time fluorescence PCR	+	1.0×10^{-6}	/	/	Milk and water	(H. Q. Yin, Jia, Yang, Wang, & Zhang, 2012)
Abrin	Au NPs; Apt	Au NPs: catalyze oxidation leading to color change; Apt: recognizes target and improves catalytic activity of Au NPs	Colorimetry	-	0.05 nM	/	0.2–17.5 nM	Milk	(Hu et al., 2015)
Gliadin	Apt	Recognizes target	Chronoamperometry	+	0.5	/	/	Soya, cake	(Amaya-González, De-Los-Santos-Álvarez, Miranda-Ordieres, & Lobo-Castañón, 2014)
Gliadin	prGO	GCE coating; binds to Abs	DPV	-	1.2	/	1.2–34	Wheat flour, pasta, Quaker oats, cereal, gluten-free wheat flour	(Chekin et al., 2016)
Gliadin	Au NPs	Bind to Abs; color source	LFA; colorimetry	+	10 mg/kg	/	/	Nine crops; 48 commercial food samples	(H. Y. Yin, Chu, Tsai, & Wen, 2016)
Gliadin	Au NPs	SPCE coating; immobilizes gliadin on electrode surface	DPV	-	8	22	0.25–250	Rice, corn, barley, rye, buckwheat, oats, mile, chestnut, chick-peas, quinoa, potato flours, durum wheat pasta, breadcrumb, crackers, and biscuits	(Manfredi et al., 2016)
Gliadin	Au NPs	Gold electrode coating; binds to Abs	QCM	+	8	11	1×10^{1}–2×10^{5}	Wheat, barley, oat, rice, foxtail millet, corn, buckwheat, and soybean; 10 commercial food samples	(Chu, Lin, Chen, Chen, & Wen, 2012)

Gliadin	QDs	Fluorophore; bind to Abs	CLSM	+	/	/	/	Dough, baked bread	(Ansari et al., 2015)
Gliadin	SIFs	Glass slide coating; signal amplifier	EFLISA	+	60	/	/	Flour	(Staiano et al., 2009)
Gliadin	IMLNs	Bind to Abs and fluorophore; signal amplifier	Fluorescence	+	600	/	/	Nine crops; 20 commercial food samples	(Chu & Wen, 2013)
Ara h1	Apt	Recognizes target	HTM	+	3 nM	4 nM	< 50 nM	Peanut butter	(Peeters et al., 2015)
Ara h 1	Apt; AuNPs	Apt: recognizes target; Au NPs: signal amplifier	FO-SPR	+	75 nM	-	0–634 nM	Candy bar	(Tran et al., 2013)
Ara h 1	Au NPs	SPCE coating; bind to Abs	LSV	+	3.8	12.6	25–2000	Cookies and chocolate	(Alves, Pimentel, Nouws, Marques, et al., 2015)
Ara h 6	Au NPs	SPCE coating; bind to Abs	LSV	+	0.27	0.88	1–100	Cookies and chocolate	(Alves, Pimentel, Nouws, Correr, et al., 2015)
DNAs									
Ara h 1 DNA	QDs–Apt–GO	QD: fluorophore; Apt: recognizes target; GO: quenching agent	Fluorescence	+	56	/	/	Biscuit	(Weng & Neethirajan, 2016)
Ara h 1 DNA	CHIT–MWCNTs	GCE coating; bind to DNA probes	Chronoamperometry	+	1.3×10^{-1} ^{7} M	/	3.91×10^{-17}–1.25×10^{-15} mol/L	Peanut	(Sun, Jia, Ji, et al., 2015)
Ara h 1 DNA	Gr–Au NPs	GCE coating; bind to DNA probes; signal amplifier	DPV	-	0.041 fM	/	1.0×10^{-16}–1.0×10^{-13} M	Peanut milk beverage	(Sun, Jia, Guan, et al., 2015)

[a]Abbreviations: LOD, limit of detection; LOQ, limit of quantification; Apt, aptamer; DPV, differential pulse voltammetry; GO, graphene oxide; poly(21dA), Au NPs, gold nanoparticles; SERS, surface-enhanced Raman scattering; EIS, electrochemical impedance spectroscopy; RBC, ricin B-chain; MB, magnetic bead; FA, fluorescence anisotropy; AVAL, N-Acryoyl-L-valine; Bpy, 4,40-bipyridyl; FONs, film-over-nanospheres; NAGEMA, N-acetyl-galactos- amine ethyl methacrylamide; RAC, ricin A-chain; MMP, magnetic microparticles; PCR, polymerase chain reaction; prGO, porous reduced graphene oxide; GCE, glassy carbon electrode; Abs, antibodies; LFA, lateral flow immunoassay; SPCE, ccreen-printed carbon electrode; QCM, quartz crystal microbalance; QDs, quantum dots; CLSM, confocal laser scanning microscopy; SIFs, silver island films; EFLISA, enhanced fluorescence linked immunosorbent assay; IMLNs, immunoliposomal nanovesicles; HTM, heat-transfer method; FO-SPR, fiber optic surface plasmon resonance; LSV, linear sweep voltammetry; CHIT, chitosan; MWCNTs, multi-walled carbon nanotubes; Gr, graphene.

[b]Positive (+) or negative (-) correlation between signal and target.

[c–e]Shown in ng/mL unless specified.

Figure(s)
Click here to download Figure(s): Revised Fig. 1.pptx

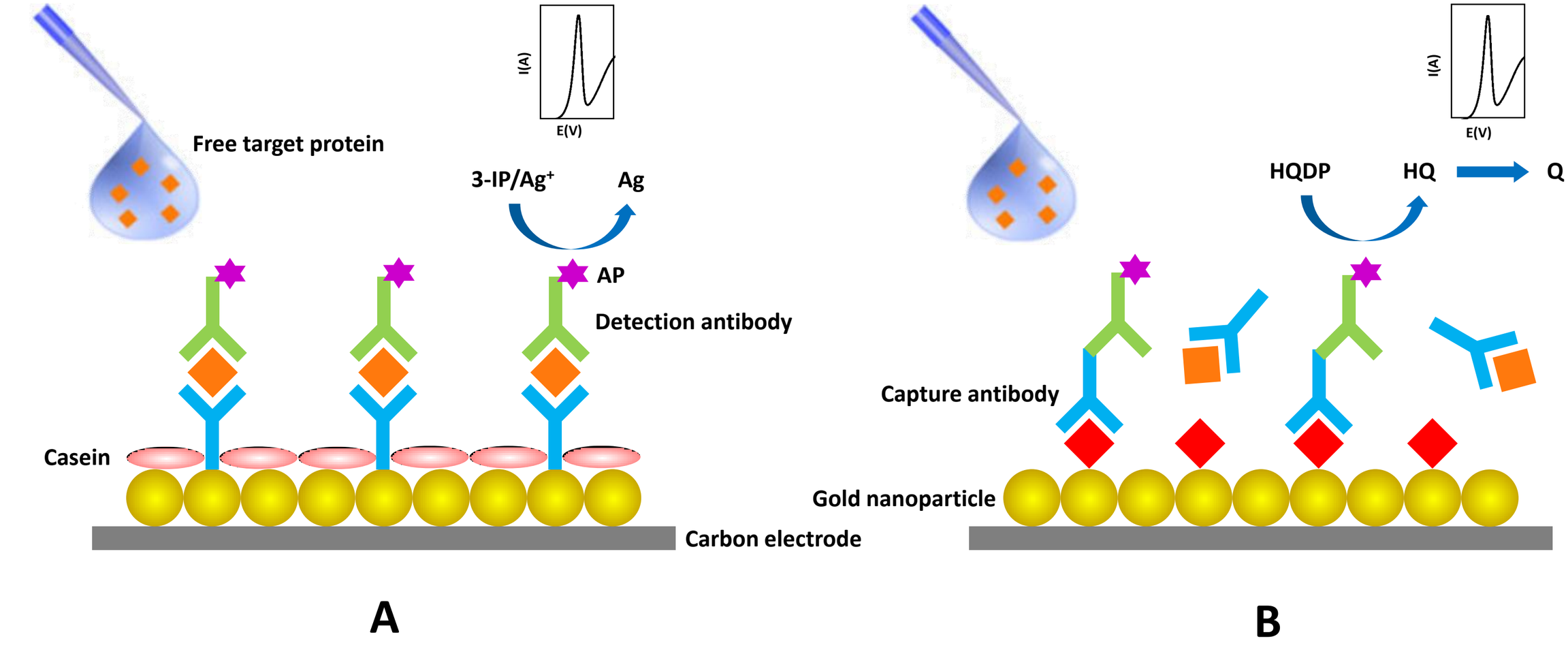

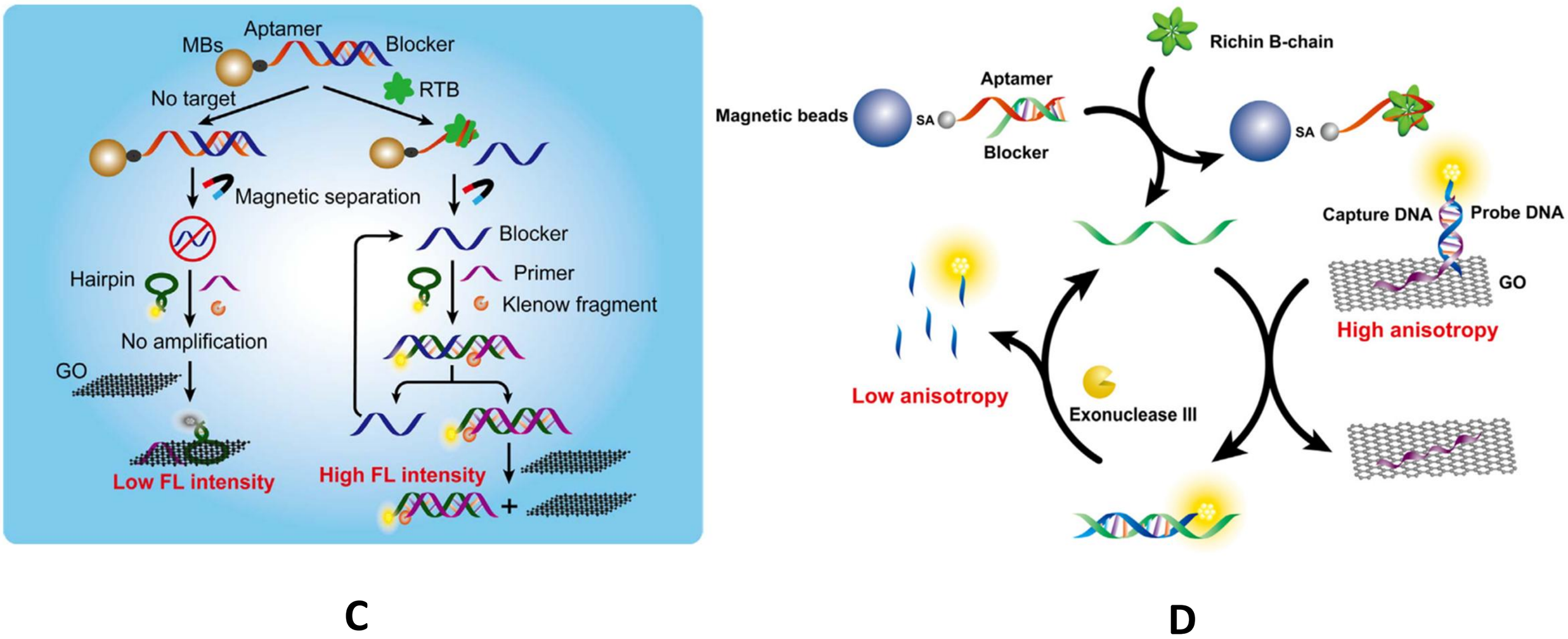

Figure(s)
Click here to download Figure(s): Revised Fig. 2.pptx


Coffee


Tea


Cola

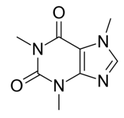
Caffeine

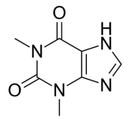
Theophylline

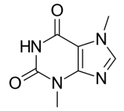
Theobromine


Strychnine tree and seeds

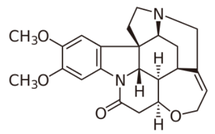
Brucine

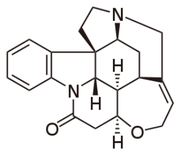
Strychnine


Poppyseed cake

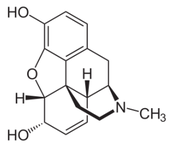
Morphine

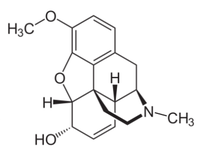
Codeine


Datura plants

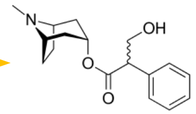
Atropine


Colchicine plants

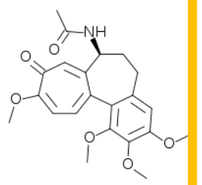
Colchicine


Cassava roots


Sweet potatoes


Peach kernels


Loquat kernels


Castor oil plant

Ricin


Rosary peas

Abrin


Wheat, barley, riye

Gluten


Peanuts

Peanut allergens

Phases / Analytes	I Sample pretreatment	II Sensor structure mediation	III Target recognition and reaction	IV Signaling
Alkaloids	Fe* CNT GO CNC Si	CNT GO* Gr Au* Cu*		QD CD
Cyanides	Fe* CNT	HA	Au* Ag* Cu*	QD Gr Au* Cu*
Proteins and corresponding DNAs	Fe*	CNT* GO* Gr Au* Ag* Al* Si*	Apt	QD GO* Gr Au* Ag* IMLN $KGdF_4:Eu^{3+}$

Supplementary Material

Click here to download Supplementary Material: Revised Synopsis.docx